AD 641337

# THE INVERSE PROBLEM OF THE ANNULAR AIRFOIL AND DUCTED PROPELLER

by

William B. Morgan and Robert G. Voigt

Distribution of this document is unlimited.

September 1966

Report 2251
S-R011 01 01
Task 0401

TABLE OF CONTENTS

| | Page |
|---|---|
| ABSTRACT | 1 |
| ADMINISTRATIVE INFORMATION | 1 |
| 1. INTRODUCTION | 1 |
| 2. LINEARIZED THEORY OF THE ANNULAR AIRFOIL | 3 |
| 2.1 BOUNDARY CONDITIONS | 4 |
| 2.2 DERIVATION OF THE EQUATION FOR THE THICKNESS DISTRIBUTION | 6 |
| 2.3 REDUCTION OF THE THICKNESS DISTRIBUTION EQUATION FOR SOLUTION ON THE IBM 7090 | 10 |
| 2.4 DERIVATION OF THE EQUATION FOR THE CAMBER DISTRIBUTION AND ANGLE OF ATTACK | 14 |
| 2.5 SIMPLIFICATION OF THE CAMBER DISTRIBUTION EQUATION FOR SOLUTION ON THE IBM 7090 | 14 |
| 3. COMPUTER PROGRAM | 17 |
| 3.1 INPUT FORMAT | 17 |
| 3.2 OUTPUT FORMAT | 19 |
| 3.3 FORTRAN LISTING | 20 |
| 4. RESULTS OF CALCULATIONS | 20 |
| 4.1 ANNULAR AIRFOIL | 20 |
| 4.2 DUCTED PROPELLER | 28 |
| CONCLUSIONS | 32 |
| ACKNOWLEDGMENTS | 32 |
| APPENDIX A - INPUT AND OUTPUT | 33 |
| APPENDIX B - FORTRAN LISTING OF COMPUTER PROGRAM | 36 |
| REFERENCES | 46 |

LIST OF FIGURES

| | Page |
|---|---|
| Figure 1 - The Annular Airfoil Coordinate System | 5 |
| Figure 2 - Delineation of the Annular Airfoil Section | 5 |
| Figure 3 - Comparison of the Computed Shapes from Theoretical and Experimental Pressure Distributions with Duct II | 25 |

Page

Figure 4 - Comparison of the Computed Shapes from Theoretical and Experimental Pressure Distributions with the BTZ Duct ........................................ 25

Figure 5 - Shape of Duct with Pressure Distribution Corresponding to a NACA 66-010 Thickness Form with and without a Propeller ........................................ 27

LIST OF TABLES

Page

Table 1 - Pressure Distribution for Duct II ...................... 21

Table 2 - Pressure Distribution for the BTZ Duct ................ 22

Table 3 - Section Shape for Duct II .............................. 23

Table 4 - Section Shape for the BTZ Duct ........................ 24

Table 5 - Pressure Distribution for a NACA 66-010 Thickness Distribution and Propeller Induced Velocities ........... 27

Table 6 - Shape of Duct with and without a Propeller ............ 29

Table 7 - Pressure Distribution of a NACA 66-010 Thickness Form with a NACA a = 0.8 Mean Line of 4 Percent Positive and Negative Camber ...................................... 31

Table 8 - Shape of Duct with a Propeller for Positive and Negative Inside Pressures ..................................... 31

## NOTATION

| | |
|---|---|
| $a$ | Duct chord |
| $b(z)$ | Annular-airfoil inner-surface ordinate |
| $c(z)$ | Mean line ordinate of the duct section measured from the nose-tail line |
| $C_p$ | $[p(x_d, z) - p_o]/\frac{1}{2}\rho V^2$, pressure coefficient |
| $E(k)$ | Complete elliptic integral of the second kind |
| $h$ | $(a/2 R_d)$ chord-diameter ratio of the duct |
| $K(k)$ | Complete elliptic integral of the first kind |
| $k$ | Modulus of the elliptic integrals |
| $p(x_d, z)$ | Local pressure on the annular airfoil |
| $p_\infty$ | Ambient pressure at infinity |
| $q$ | Ring-source strength |
| $R_d$ | Duct radius |
| $(r, \phi, z)$ | Cylindrical coordinates |
| $s(z)$ | Half-thickness ordinate of the duct section |
| $u(z)$ | Annular-airfoil outer-surface ordinate |
| $V$ | Free-stream velocity |
| $w_a$ | Axial component of induced velocity |
| $w_o$ | Component of free-stream velocity in direction of duct axis |
| $w_r$ | Radial component of induced velocity |
| $w_{x_d}$ | Taylor wake fraction at the duct |
| $x$ | Radial coordinate nondimensionalized by the propeller radius |
| $\alpha$ | Angle of attack of a duct section |
| $\gamma$ | Ring-vortex strength |
| $\rho$ | Mass density |

Subscripts

| | | | |
|---|---|---|---|
| d | Duct | q | Ring source |
| p | Propeller | $\gamma$ | Ring vortex |

Note: Many functions are defined in the text.

## ABSTRACT

A computer program is presented that calculates the annular airfoil shape from a given pressure distribution. A brief review of the theory of the inverse problem of the annular airfoil is also presented. The distortion of the duct shape by the presence of an axisymmetric body or a propeller may be taken into consideration. Calculations show that for a given pressure distribution, the propeller loading and location affect the duct shape.

## ADMINISTRATIVE INFORMATION

This work was covered by Subproject S-R011 01 01, Task 0401, under the Bureau of Ships In-House Independent Research Program.

## 1. INTRODUCTION

Annular airfoils have been used for many years[1] as shroud rings around marine propellers. These ducts have been used for the acceleration of the velocity at the propeller (Kort nozzles); this has the effect of increasing the efficiency when the unit is heavily loaded. Impetus in the last few years has been given for their use to increase the thrust of propellers during takeoff for short and vertical takeoff aircraft. Also, in naval architecture, ducts that decelerate the flow at the propeller (pumpjets) have found application for delaying cavitation on the propeller.

A number of experimental and theoretical investigations have been conducted on the annular airfoil and the ducted propeller. A general review of these studies has been made by Sacks and Burnell[2] so only the pertinent and more recent results will be reviewed here. In most of the theoretical investigations, a distribution of ring vortices and ring sources is used which lie on a cylinder of diameter representative of the duct and of length equal to the duct length.[3-7] The use of this mathematical model implies that the boundary conditions are linearized and are satisfied on the representative cylinder and not on the duct surface. A

---

[1]References are listed on page 46.

nonlinear theory for the annular airfoil has been presented by Chaplin[8] where the annular airfoil is represented by a system of ring vortices lying on the surface of the airfoil. He includes both the static and the free-flight cases.

In the references just given, the direct problem of the annular airfoil is considered, i.e., given an annular airfoil shape, determine the pressure distribution and forces on the duct. Reference 9, however, presents the theory for the inverse problem, i.e., given a pressure distribution, determine the annular airfoil shape.

Both the direct and the inverse problems require the solution of a singular integral equation, the first for the ring vortex distribution, and the second for the ring source distribution. Another approach given in References 10, 11,* 12, and 13 is to assume the ring vortex strength and, if the effect of thickness is considered, to assume the thickness distribution. The disadvantages of this procedure are that the circulation must be specified, which is not a physical property of the annular airfoil, and it is not possible to tell a priori whether the pressure distribution or the shape will be satisfactory.

The usefulness of the inverse problem is to delineate annular airfoil shapes which will operate satisfactorily for a given flow condition. This is to say that in the presence of a propeller producing a given thrust, a duct shape can be determined which will not separate in air or water, nor cavitate in water. Both separation and cavitation are, of course, real fluid effects, so some criteria for the pressure distribution must be specified which will indicate satisfactory operation. For instance, for cavitation a minimum pressure coefficient would be assumed, and for separation a maximum rate of change of the pressure coefficient would be assumed.

This report presents a computer program and representative type calculations based on the inverse problem presented in Reference 9. The program allows the inclusion of an axisymmetric perturbation velocity so

*There is a difference in definition of the direct and inverse problem between References 9 and 11.

that the duct shape can be determined in the presence of a propeller or any body which is axisymmetric to the duct. Only the average effect of the propeller can be considered, however, as including the effect of a finite number of blades would imply that the annular airfoil can change shape as the propeller rotates.

The following discussion is divided into three main sections. The development of the theory is reviewed briefly, then the computer program is described and presented, and finally, computed duct shapes are presented for comparison. Calculations are also included which show how the shape of the duct changes with variation in propeller loading.

## 2. LINEARIZED THEORY OF THE ANNULAR AIRFOIL

Although the linearized theory of the annular airfoil has been adequately developed in the reference cited, a brief sketch of the development will be repeated here for the sake of completeness.

As was stated in the Introduction, the method of singularities is used for the representation of the flow field about the annular airfoil. The mathematical model used is a distribution of ring vortices and ring sources lying on a cylinder having a length equal to the length of the annular airfoil and a diameter representative of the diameter of the annular airfoil. The use of this model for the inverse problem necessitates a number of assumptions:

1. The real fluid is inviscid and incompressible and no separation occurs on the annular airfoil.

2. Body forces such as gravity are negligible.

3. The freestream flow is axisymmetric and steady, but an axisymmetric disturbing velocity may exist. An implication here is that the static condition is not considered.

4. The annular airfoil is axisymmetric and has finite length.

5. The distribution of ring vortices and ring sources along a cylinder does, indeed, represent the annular airfoil. This implies that the boundary conditions are linearized.

## 2.1 BOUNDARY CONDITIONS

The coordinate system used is a cylindrical system $(r, \phi, z)$ whose polar-axes are located at the trailing edge and z-axis coincides with the centerline of the annular airfoil. For convenience, the axial coordinate is nondimensionalized by the chord a, and the radial coordinate by the representative radius $R_d$, of the annular airfoil. Figure 1 gives the coordinate system and Figure 2 is a delineation of the system.

The pressure distribution on the annular airfoil is assumed known and the cross section of the airfoil is calculated in terms of a camber distribution c(z), a thickness distribution s(z), and an angle of attack $\alpha$, as follows:

$$\begin{aligned} u'(z) &= c'(z) + s'(z) + \tan\alpha \\ b'(z) &= c'(z) - s'(z) + \tan\alpha \end{aligned} \qquad [2.1.1]$$

where $u'(z)$ is the slope of the outer surface and $b'(z)$ is the slope of the inner surface of the annular airfoil.

The boundary conditions to be satisfied are that the normal velocity must be zero on the surface of the annular airfoil and the Kutta condition must be satisfied at the trailing edge. In linearized theory[14] this means that the radial velocity at the representative cylinder must be equal to the slope of the section, or

$$\frac{w_r}{V}(x_d \pm 0, z) = -(1 - w_{x_d})\,[c'(z) \pm s'(z) + \tan\alpha] \qquad [2.1.2]$$

where for convenience for the naval architect the wake $(1 - w_{x_d}) = \frac{w_o}{V}$ is introduced. At the trailing edge the radial velocity is zero, or

$$\frac{w_r}{V}(x_d \pm 0, 0) = 0$$

In the symbol $\pm$, the + sign denotes the outer surface of the annular airfoil and the - sign denotes the inner surface.

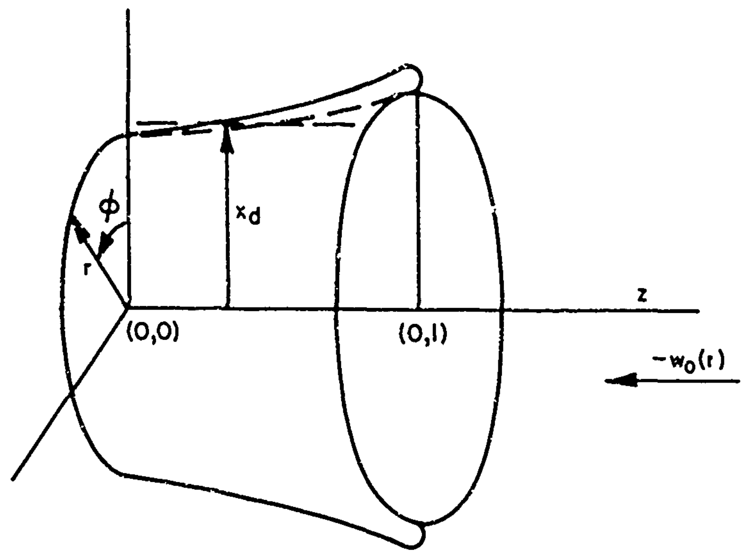


Figure 1 - The Annular Airfoil Coordinate System

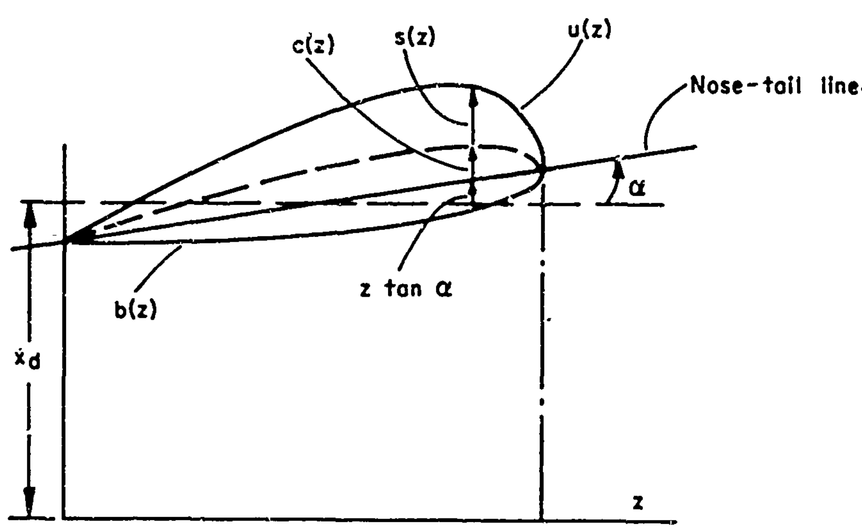


Figure 2 - Delineation of the Annular Airfoil Section

## 2.2 DERIVATION OF THE EQUATION FOR THE THICKNESS DISTRIBUTION

To calculate the thickness distribution, camber distribution, and the angle of attack of the annular airfoil from the pressure distribution, it is necessary to obtain the strength of the ring vortices and ring sources. The ring vortex and ring source strengths must be of sufficient magnitude that they induce radial velocities that satisfy the given boundary conditions. By substituting the equations for the radial velocity induced by the ring vortices and sources into Equation [2.1.1], an expression for the slope of the thickness distribution is obtained in terms of known quantities.

The nondimensional elementary circulation of the ring vortices is represented by $\gamma(z)$ and the strength of the ring sources by $q(z)$. Since the velocities are linear, they are additive; thus the radial velocities along the annular airfoil are found to be

$$\frac{w_r}{V}(x_d \pm 0,\ z) = \left[\frac{w_r}{V}(x_d,\ z)\right]_\gamma + \left[\frac{w_r}{V}(x_d \pm 0,\ z)\right]_q + \left[\frac{w_r}{V}(x_d,\ z)\right]_p \qquad (0 \leq z \leq 1) \qquad [2.2.1]$$

$[w_r\ (x_d,\ z)]_\gamma$ = the radial velocity induced on the annular airfoil by the ring-vortex system,

$[w_r\ (x_d \pm 0,\ z)]_q$ = the radial velocity induced on the annular airfoil by the ring-source system, and

$[w_r\ (x_d,\ z)]_p$ = the radial velocity induced on the annular airfoil by a propeller or any other singularities in the flow.

The expressions for these velocity components have been derived in Reference 14 and are as follows:

$$\left[\frac{w_r}{V}(x_d,\ z)\right]_\gamma = -\frac{1}{4\pi}\int_0^1 \frac{\gamma(z')\ k}{(z - z')}\left\{4h^2\ (z - z')^2\ [K(k) - E(k)] - 2E(k)\right\}dz' \qquad [2.2.2]$$

$$\left[\frac{w_r}{V}(x_d \pm 0,\ z)\right]_q = \frac{h}{2\pi}\int_0^1 q(z')k\ [K(k) - E(k)]\ dz' \pm \frac{1}{2}q(z) \qquad [2.2.3]$$

where $h = \frac{a}{2R_d}$, $k^2 = \frac{1}{h^2(z - z')^2 + 1}$, and $K(k)$ and $E(k)$ are complete elliptic integrals of the first and second kind, respectively. The symbol $⨍$ denotes a Cauchy principal value integral.

By substituting these expressions in Equations [2.1.2] and [2.2.1], the following equation is obtained.

$$-\frac{1}{4\pi}⨍_0^1 \frac{\gamma(z')}{(z-z')}\ k\ \{4h^2(z-z')^2\ [K(k) - E(k)] - 2E(k)\}\ dz'$$

$$+\frac{h}{2\pi}\int_0^1 q(z')k\ [K(k) - E(k)]\ dz' \pm \frac{1}{2}q(z) =$$

$$-\left(1-w_{x_d}\right)[c'(z) \pm s'(z) + \tan\alpha] - \left[\frac{w_r}{V}(x_d,\ z)\right]_p \qquad [2.2.4]$$

Since the integrals occurring in this equation have only one sign and since the radial velocity induced by the propeller on the annular airfoil does not change sign from one side of the foil to the other, it may be concluded that the $\pm$ signs go with the $\mp$ signs and hence

$$q(z) = -\ 2\left(1 - w_{x_d}\right)s'(z) \qquad [2.2.5]$$

This equation gives the relationship between the ring source strength and the slope of the thickness distribution. The next step is to find the total velocity tangent to the airfoil in terms of the ring vortex strength, ring source strength, and the strength of any other singularity present in the flow such as a propeller. Since the annular airfoil is theoretically replaced by a cylinder, the velocity in question is just the axial velocity. The pressure distribution is related to the induced velocities by means of the linearized Bernoulli equation, i.e.,

$$C_p = \frac{p(x_d,\ z) - p_\infty}{\frac{1}{2}\rho\ V^2} \approx 2\frac{w_a}{V}(x_d,\ z) \qquad [2.2.6]$$

where $p(x_d, z)$ = the local pressure on the annular airfoil,

$p_\infty$ = ambient pressure at infinity,

$w_a(x_d, z)$ = the axial component of induced velocity on the annular airfoil, and

$\rho$ = the mass density.

Within linearized theory all velocities are additive; thus the total axial velocity is given by

$$\left[\frac{w_a}{V}\right]_{total} = \left[\frac{w_a(z)}{V}\right]_\gamma + \left[\frac{w_a(z)}{V}\right]_q + \left[\frac{w_a(z)}{V}\right]_p - \frac{w_o}{V} \qquad [2.2.7]$$

where $\left[\frac{w_a(z)}{V}\right]_\gamma$ = the axial velocity induced on the annular airfoil by the ring-vortex system,

$\left[\frac{w_a(z)}{V}\right]_q$ = the axial velocity induced on the annular airfoil by the ring-source system,

$\left[\frac{w_a(z)}{V}\right]_p$ = the axial velocity induced on the annular airfoil by a propeller or any other singularity in the flow, and

$\left[\frac{w_o}{V}\right]$ = speed of advance of the duct.

From Equation [2.2.2] the perturbation velocity distribution $w_a$ is obtained as

$$\frac{w_a(z)}{V} = \left[\frac{w_a(z)}{V}\right]_{total} + \left[\frac{w_o}{V}\right] = \left[\frac{w_a(z)}{V}\right]_\gamma + \left[\frac{w_a(z)}{V}\right]_q + \left[\frac{w_a(z)}{V}\right]_p \qquad [2.2.8]$$

It is, of course, not possible to determine the section shape in the presence of a propeller with a finite number of blades since the pressure distribution is essentially time-dependent; however, it is possible to consider the average effect of the propeller which corresponds to an infinitely bladed propeller. Under this restriction the duct circulation distribution, defined as $\gamma(z)$, is a function of z only and justifies the use of the following relationship from Reference 14 for the axial velocity induced on the duct by the ring vortex distribution and ring source distribution, respectively:

$$\left[\frac{w_a\left(x_d \pm 0,\ z\right)}{V}\right]_\gamma = \frac{h}{2\pi}\int_0^1 \gamma(z') \; k \; [K(k) - E(k)] \; dz' \mp \frac{1}{2}\gamma(z) \quad [2.2.9]$$

$$\left[\frac{w_a\left(x_d,\ z\right)}{V}\right]_q = \frac{2}{\pi}\oint_0^1 \frac{q(z')}{(z-z')} \; k \; E(k) \; dz' \qquad [2.2.10]$$

or in terms of Equation [2.2.5]

$$\left[\frac{w_a\left(x_d,\ z\right)}{V}\right]_q = -\frac{\left(1-w_{x_d}\right)}{\pi}\oint_0^1 \frac{s'(z')}{(z-z')} \; k \; E(k) dz'$$

If Equations [2.2.9] and [2.2.10] are substituted into Equation [2.2.8],

$$\left[\frac{w_a(z)}{V}\right]_\pm = \frac{1}{2} C_p = \frac{h}{2\pi}\int_0^1 \gamma(z') \; k \; [K(k) - E(k)] \; dz' \mp \frac{1}{2}\gamma(z)$$

$$- \frac{\left(1-w_{x_d}\right)}{\pi}\oint_0^1 \frac{s'(z') \; k \; E(k)}{(z - z')} \; dz' + \left[\frac{w_a(z)}{V}\right]_p \qquad [2.2.11]$$

A mean velocity is defined as

$$\left[\frac{w_a(z)}{V}\right]_{mean} = \frac{1}{2}\left\{\left[\frac{w_a(z)}{V}\right]_+ + \left[\frac{w_a(z)}{V}\right]_-\right\} = \frac{1}{4}\left[C_{p+} + C_{p-}\right] \qquad [2.2.12]$$

and substitution of Equation [2.2.11] into this equation gives

$$\left[\frac{w_a(z)}{V}\right]_{mean} = \frac{h}{2\pi}\oint_0^1 \gamma(z') \; k \; [K(k) - E(k)] \; dz'$$
$$- \frac{\left(1-w_{x_d}\right)}{\pi}\oint_0^1 \frac{s'(z') \; k \; E(k)}{(z - z')} \; dz' + \left[\frac{w_a(z)}{V}\right]_p \qquad [2.2.13]$$

A velocity difference is also defined as

$$\left[\frac{w_a(z)}{V}\right]_{diff} = \left\{\left[\frac{w_a(z)}{V}\right]_+ - \left[\frac{w_a(z)}{V}\right]_-\right\} = \frac{1}{2}\left[C_{p+} - C_{p-}\right] \qquad [2.2.14]$$

and substitution into Equation [2.2.11] gives

$$\left[\frac{w_a(z)}{V}\right]_{diff} = - \gamma(z) \qquad [2.2.15]$$

Since $\left[\frac{w_a(z)}{V}\right]_{mean}$ and $\left[\frac{w_a(z)}{V}\right]_{diff}$ are known from the pressure distribution, substitution of Equation [2.2.15] into [2.2.13] gives a singular integral equation for the slope of the thickness distribution in terms of known quantities:

$$\oint_0^1 \frac{s'(z)\ k\ E(k)}{(z - z')}\ dz' = \frac{-\pi}{\left(1-w_{x_d}\right)} \left\{\left[\frac{w_a(z)}{V}\right]_{mean} - \left[\frac{w_a(z)}{V}\right]_p\right\}$$
$$- \frac{h}{2\left(1-w_{x_d}\right)} \int_0^1 \left[\frac{w_a(z)}{V}\right]_{diff} k\ [K(k) - E(k)]\ dz' \qquad [2.2.16]$$

## 2.3 REDUCTION OF THE THICKNESS DISTRIBUTION EQUATION FOR SOLUTION ON THE IBM 7090

To facilitate solving the expression for the slope of the thickness distribution, Equation [2.2.16] is reduced to a Fredholm equation of the second kind by using a method given by Muskhelishvili.[15] The resulting equation contains singularities and is handled by a method discussed in Reference 16.

For convenience, Equation [2.2.16] is rewritten as

$$\oint_0^1 g(z - z')\ \frac{s'(z')}{(z - z')}\ dz' = H(z) \qquad [2.3.1]$$

where $g(z - z') = k\ E(k)$

and $H(z) = - \frac{h}{2\left(1-w_{x_d}\right)} \int_0^1 \left[\frac{w_a(z')}{V}\right]_{diff} k\ [K(k) - E(k)]\ dz' -$

$$\frac{\pi}{\left(1-w_{x_d}\right)} \left\{\left[\frac{w_a(z)}{V}\right]_{mean} - \left[\frac{w_a(z)}{V}\right]_p\right\}$$

Now the term $g(0)\ \frac{s'(z')}{(z - z')}$ is added to and subtracted from the integrand of Equation [2.3.1] giving

$$g(0) \oint_0^1 \frac{s'(z')}{(z - z')}\ dz' + \int_0^1 [g(z - z') - g(0)]\ \frac{s'(z')}{(z - z')}\ dz' = H(z)$$

or since $g(0) = 1$

$$\oint_0^1 \frac{s'(z')}{(z - z')} dz' = H(z) - \int_0^1 [g(z - z') - 1] \frac{s'(z')}{(z - z')} dz' \equiv \bar{H}(z) \quad [2.3.2]$$

This equation is now in the form of a Cauchy integral equation because the right side is free from singularities. As found in Reference 9, this equation has a unique inverse given by

$$s'(z) = \frac{1}{\pi \sqrt{z (1 - z)}} \left\{ \frac{1}{\pi} \oint_0^1 \frac{\sqrt{z (1 - z)}}{(z' - z)} \bar{H}(z') dz' + 2 \int_0^1 s'(z') dz' \right\}$$

Since the airfoil section must be closed, $\int_0^1 s'(z') dz' = 0$ and by using equation [2.3.2] a Fredholm equation of the second kind is obtained

$$s'(z) = \frac{1}{\sqrt{z (1 - z)}} \left\{ - f(z) + \frac{1}{\pi^2} \int_0^1 G(z, z') s'(z') dz' \right\} \quad [2.3.3]$$

where

$$f(z) = -\frac{1}{\pi^2} \oint_0^1 \frac{\sqrt{z' (1 - z')}}{(z' - z)} H(z') dz'$$

and

$$G(z, z') = \frac{1}{\pi^2} \oint_0^1 \frac{\sqrt{z'' (1 - z'')} [1 - g(z' - z'')]}{(z'' - z) (z'' - z')} dz''$$

Equation [2.3.3] cannot be handled in its present form since there exists a square root singularity at $z = 0$ and $z = 1$. To remove the singularities and, as will be seen later, to facilitate evaluation of $f(z)$ and $G(z, z')$ the following change of variable is used:

$$z = \frac{1}{2} (1 + \cos \theta)$$

Since

$$s'(z) = - \frac{2 s'[(1/2) (1 + \cos \theta)]}{\sin \theta}$$

the following equation is obtained from Equation [2.3.3]:

$$s^{*'}(\theta) = f^{*}(\theta) + \int_0^1 G^{*}(\theta, \theta') s^{*'}(\theta') d\theta' \quad [2.3.4]$$

where

$$f^*(\theta) = -\frac{1}{2\pi^2}\int_0^\pi \frac{H^*(\theta')\sin^2\theta'\,d\theta'}{(\cos\theta' - \cos\theta)}$$

$$G^*(\theta,\theta') = \frac{1}{\pi^2}\int_0^\pi \frac{[1 - k\,E(k)]\sin^2\theta''\,d\theta''}{(\cos\theta'' - \cos\theta)\,(\cos\theta'' - \cos\theta')}$$

and

$$k^2 = \frac{1}{\frac{1}{4}h^2\,(\cos\theta'' - \cos\theta')^2 + 1}$$

The symbol * is used to simplify notation; for example,

$$f(z) = f[(1/2)\,(1 + \cos\theta)] \equiv f^*(\theta)$$

The integrals $f^*(\theta)$ and $G^*(\theta, \theta')$ are Cauchy principal value integrals and to evaluate, part of the integrand of each is expanded in a Fourier cosine series, i.e.,

$$H^*(\theta')\sin^2\theta' = a_o + \sum_{n=1}^{\infty} a_n \cos\theta'$$

where

$$a_o = \frac{1}{\pi}\int_0^\pi H^*(\theta')\sin^2\theta'\,d\theta'$$

$$a_n = \frac{2}{\pi}\int_0^\pi H^*(\theta')\sin^2\theta'\cos n\theta'\,d\theta'$$

then

$$f^*(\theta) = \frac{1}{2\pi}\sum_{n=1}^{\infty} a_n \frac{\sin n\theta}{\sin\theta} \qquad [2.3.5]$$

and

$$\frac{[1-k\,E(k)]\sin^2\theta''}{\text{con}\,\theta''\ \cos\theta'} = b_o(\theta') + \sum_{n=1}^{\infty} b_n(\theta')\cos n\theta''$$

where

$$b_o(\theta') = \frac{1}{\pi}\int_0^\pi \frac{[1-k\,E(k)]\sin^2\theta''}{\cos\theta'' - \cos\theta'}\,d\theta''$$

$$b_n(\theta') = \frac{2}{\pi}\int_0^\pi \frac{[1-k\,E(k)]\sin^2\theta''}{\cos\theta'' - \cos\theta'}\cos n\theta''\,d\theta''$$

then

$$G^*(\theta, \theta') = \frac{1}{\pi} \sum_{n=1}^{\infty} b_n(\theta') \frac{\sin n\theta}{\sin \theta} \qquad [2.3.6]$$

The kernel $G^*(\theta, \theta')$ is now of the degenerate type and Equation [2.3.4] can be solved by the method applicable to this type of kernel. Details of the method are given in Reference 17. If this procedure is followed, the following equation for the slope of the thickness distribution is obtained.

$$s^{*\prime}(\theta) = f^*(\theta) + \frac{1}{\pi} A_1 + \frac{1}{\pi} A_2 \frac{\sin 2\theta}{\sin \theta} + \ldots + \frac{1}{\pi} A_n \frac{\sin n\theta}{\sin \theta} \qquad [2.3.7]$$

where

$f^*(\theta)$ is given by Equation [2.3.5].

And $A_n$ is given by the following set of simultaneous equations:

$$\begin{array}{l} A_1 (1 - c_{11}) - A_2 c_{12} - \ldots - A_n c_{1n} = d_1 \\ - A_1 c_{21} + A_2 (1 - c_{22}) - \ldots - A_n c_{2n} = d_2 \\ \cdot \quad \cdot \quad \cdot \quad \cdot \quad \cdot \quad \cdot \quad \cdot \quad \cdot \\ \cdot \quad \cdot \quad \cdot \quad \cdot \quad \cdot \quad \cdot \quad \cdot \quad \cdot \\ - A_1 c_{n1} - A_2 c_{n2} - \ldots + A_n \left(1 - c_{nn}\right) = d_n \end{array} \qquad [2.3.8]$$

where

$$c_{ij} = \frac{1}{\pi} \int_0^{\pi} b_i(\theta') \frac{\sin j\theta'}{\sin \theta'} d\theta' \quad (i,j = 1,2,3 \ldots n)$$

$$d_i = \int_0^{\pi} b_i(\theta') f^*(\theta') d\theta' \quad (i = 1,2,3 \ldots n)$$

Expression [2.3.7] is the expression solved on the computer with a finite sum replacing the infinite sum in Equation [2.3.5]. The $c_{ij}$'s and $d_i$'s may be evaluated as given, so the $A_i$'s follow immediately from [2.3.8]. However, to evaluate the $a_n$'s in Equation [2.3.5], the singularity must be removed in $H^*(\theta')$. This is accomplished by using the change of variables $t^3 = \theta'' - \theta'$ where $\theta''$ is the variable of integration for $H^*(\theta')$. The thickness distribution now follows immediately by integrating Equation [2.3.7] from 0 to $\theta$.

## 2.4 DERIVATION OF THE EQUATION FOR THE CAMBER DISTRIBUTION AND ANGLE OF ATTACK

To calculate the camber distribution and the angle of attack, it is only necessary to integrate Equation [2.2.4] after substituting for the known quantities. Equation [2.2.4] is rewritten and substitution for the source strength q and vortex strength $\gamma$ is made from Equations [2.2.5] and [2.2.15], respectively.

$$c'(z) + \tan\alpha = -\frac{h^2}{\pi\left(1 - w_{x_d}\right)} \int_0^1 \left[\frac{w_a(z')}{V}\right]_{diff} (z - z')\, k\, [K(k) - E(k)]dz'$$

$$+ \frac{1}{2\pi\left(1 - w_{x_d}\right)} \oint_0^1 \left[\frac{w_a(z')}{V}\right]_{diff} \frac{k\, E(k)}{(z - z')}\, dz' \qquad [2.4.1]$$

$$+ \frac{h}{\pi} \oint_0^1 s'(z')\, k[K(k) - E(k)]dz' - \frac{1}{\left(1 - w_{x_d}\right)} \left[\frac{w_r}{V}\left(x_d, z\right)\right]_p$$

If Equation [2.4.1] is integrated with respect to z from 0 to 1, the tangent of the angle of attack is obtained since $\int_0^1 c'(z)\, dz = 0$. Equation [2.4.1] is the desired expression for the slope of the camber distribution.

## 2.5 SIMPLIFICATION OF THE CAMBER DISTRIBUTION EQUATION FOR SOLUTION ON THE IBM 7090

To facilitate solving the expression for the slope of the camber distribution, Equation [2.4.1], a change of variable is made. The resulting equation contains various singularities which are handled by a method suggested in Reference 15..

With $z = \frac{1}{2}(1 + \cos\theta)$ Equation [2.4.1] has the form

$$\frac{-2c^{*\prime}(\theta)}{\sin\theta} + \tan\alpha = -\frac{h^2}{4\pi\left(1 - w_{x_d}\right)} \cdot \int_0^1 \left[\frac{w_a^*(\theta')}{V}\right]_{diff} (\cos\theta - \cos\theta')$$

$$\cdot\, k[K(k) - E(k)]\, \sin\theta'\, d\theta'$$

$$+ \frac{1}{2\pi\left(1 - w_{x_d}\right)} \oint_0^1 \left[\frac{w_a^*(\theta)}{V}\right]_{diff} \frac{k\, E(k)\, \sin\theta'\, d\theta'}{\cos\theta - \cos\theta'}$$

$$- \frac{h}{\pi} \int_0^{\pi} s^{*'}(\theta') \, k[K(k) - E(k)] \, d\theta' \qquad [2.5.1]$$

$$\frac{1}{\left(1 - w_{x_d}\right)} \left[\frac{w_r^{*}(x_d, \theta)}{V}\right]_p$$

where the notation * and the form of k are given in Equation [2.3.4].

Because of the presence of the term cos θ - cos θ′ the first integral in Equation [2.5.1] has no singularities and may, therefore, be evaluated immediately by use of the computer.

The second integral in Equation [2.5.1] is a Cauchy principal value integral and is first simplified by a technique given in Reference 15; the term

$$\left[\frac{w_a^{*}(\theta)}{V}\right]_{diff} \frac{\sin \theta}{\cos \theta - \cos \theta'}$$

is added to and subtracted from the integrand:

$$\frac{1}{2\pi\left(1 - w_{x_d}\right)} \left\{ \int_0^{\pi} \frac{\left[\frac{w_a^{*}(\theta)}{V}\right]_{diff} kE(k) \sin \theta' - \left[\frac{w_a^{*}(\theta)}{V}\right]_{diff} \sin \theta}{\cos \theta - \cos \theta'} \, d\theta' \right. \qquad [2.5.2]$$

$$\left. + \left[\frac{w_a^{*}(\theta)}{V}\right]_{diff} \sin \theta \oint_0^{\pi} \frac{d\theta'}{\cos \theta - \cos \theta'} \right\}$$

The second integral in this expression is zero so only the first integral needs to be considered.

The behavior of the integrand is investigated as $\theta' \to \theta$ by L'Hospital's rule and the following limit is obtained:

$$\frac{\frac{d}{d\theta} \left\{ \left[\frac{w_a^{*}(\theta)}{V}\right]_{diff} \sin \theta \right\}}{\sin \theta} \qquad [2.5.3]$$

Now with this knowledge of the behavior of the integrand of expression

[2.5.2], the second integral in Equation [2.5.1] is evaluated by integrating [2.5.2] on the computer and using [2.5.3] evaluated numerically for the value of the integrand at $\theta' = \theta$.

The third integral in Equation [2.5.1] is simplified as follows. First this equation is integrated by parts with

$$u = k\ [K(k) - E(k)]$$

$$dv = s^{*\prime}(\theta')\ d\theta'$$

Then $v = s^*(\theta')$ and after differentiation and considerable simplification (see page 107 of Reference 18),

$$du = -\ k^3 \frac{h^2}{4}\ (\cos\theta - \cos\theta')\ \sin\theta' \left\{ K(k) - E(k) + E(k)\ \frac{k^2}{1-k^2} \right\} d\theta'$$

Now by using the fact that $s^*(\theta')\ \big|_{\theta'=0} = s^*(\theta')\big|_{\theta'=\pi} = 0$ the following equation is obtained

$$\int_0^\pi s^{*\prime}(\theta')\ k[K(k) - E(k)]\ d\theta' = \frac{h^2}{4} \int_0^\pi s^*(\theta')\ k^3\ (\cos\theta - \cos\theta')$$

$$\sin\theta'\ [K(k) - E(k)]\ d\theta'$$

$$+ \oint_0^\pi \frac{s^*(\theta')\ k^3\ \sin\theta'\ E(k)}{\cos\theta - \cos\theta'}\, d\theta' \qquad [2.5.4]$$

The first integral on the right-hand side of Equation [2.5.4] can be evaluated on the computer immediately; the second, however, must be simplified as in the second integral of Equation [2.5.1]. Thus the term

$$\frac{s^*(\theta)\ \sin\theta}{\cos\theta - \cos\theta'}$$

is added to and subtracted from the integrand obtaining

$$\int_0^\pi \frac{s^*(\theta')\ k^3\ \sin\theta'\ E(k) - s^*(\theta)\ \sin\theta}{\cos\theta - \cos\theta'}\ d\theta'$$

since, as before, $\oint_0^\pi \dfrac{d\theta'}{\cos\theta - \cos\theta'}\ d\theta' = 0$

As in the integral [2.5.2] the behavior of the integrand as $\theta' \to \theta$ is investigated and $s^{*\prime}(\theta) + s^{*}(\theta) \cot \theta$ is obtained as the value of the limit. Thus the complete expression [2.5.4] may now be evaluated numerically.

All three integrals of Equation [2.5.1] are now in a form suitable for numerical evaluation, so tan $\alpha$ may be found by integrating [2.5.1] from 0 to $\pi$ and recalling that $\int_0^\pi c^{*\prime}(\theta')d\theta' = 0$. The slope of the camber distribution then follows immediately, and integration from 0 to $\theta$ gives the camber distribution.

## 3. COMPUTER PROGRAM

The calculations based on the theory presented in Section 2 have been programmed for the IBM 7090 high-speed computer. Input consists of a pressure distribution on the inner and outer surfaces of the annular airfoil, the chord-diameter ratio of the annular airfoil, and a wake fraction. It is also possible to make calculations with a propeller or any axisymmetric body located in the annular airfoil; however, axial and radial components of the induced velocity must be included.

The output consists of the thickness distribution, the camber distribution, and the angle of attack of the annular airfoil. It takes approximately 8 minutes on the IBM 7090 high-speed computer to obtain these results.

The input-output format and the FORTRAN listing of the computer program are discussed in the following sections.

### 3.1 INPUT FORMAT

The first input card contains an integer which represents the number of cases to be run. This number is entered in Columns 1-4 under an I4 format. The only limit to the number of cases to be run is a consideration of computer time.

The second card is a problem identification card. A one (1) must appear in Column 1 and any alphanumeric characters may appear in Columns 2 through 72. Even if no identification is desired, the card must be included with a one (1) in Column 1.

The third card contains 10 parameters in the format 2F10.6,8I4. They are as follows:

1. The chord-diameter ratio.

2. The wake fraction.

3. The maximum number of Fourier coefficients to be allowed in the evaluation of the kernel function $G^*(\theta,\theta')$, Equation [2.3.4]. The user may specify any number not exceeding 40. The program calculates Fourier coefficients until either a convergence criteria of $10^{-6}$ has been met or the number of coefficients equals the number specified in this parameter. The program normally uses between 20 and 25 terms so the user may specify 40 since only as many terms are calculated as are needed.

4. The number of ordinates used in the integral evaluations. The integrations are performed using Simpson's rule so this number must be odd. The maximum allowed by the dimension of the program is 101. Normally, a value of 51 is more than adequate and if time is a factor, 25 would probably suffice.

5. The number of input pressure data points. This number may not exceed 37. If possible, to facilitate interpolation, the user should specify closer spaced data in regions where the pressure curves have steep slopes.

6. The number of points to be used for the harmonic analysis of the Cauchy principle value integral $f^*(\theta)$, Equation [2.3.4]. The maximum allowed by the dimension of the program is 200 and this is also the suggested value.

7. The number of harmonics used in the harmonic analysis described in parameter 6. This number must be strictly less than one-half the number specified in 6. Normally, a value of 45 is more than adequate.

8. The maximum number of ordinates used in integrating $s^{*\prime}(\theta)$ and $c^{*\prime}(\theta)$ to obtain the thickness and camber distributions. The number must be greater than or equal to 51 and must be odd. A value of 61 has proven to be satisfactory. There is no upper bound on this parameter.

9. The parameter signifying the presence of a propeller or any axisymmetric body in the annular airfoil. The parameter must have the values:

1 if a propeller or body is present,

2 if a propeller or body is not present.

10. The parameter controlling the punching of one-half the thickness and camber distributions on IBM cards by the machine. This parameter must have the values:

1 if no data is to be punched,

2 if data is to be punched.

The format of the punched data is discussed in the following paragraphs. A discussion of the effects of varying parameters 3 and 7 may be found in Reference 16.

The fourth card is the first card containing pressure data. The value of parameter 5 on the third card determines the number of these cards. Each card contains the abscissa of the pressure distribution and four pressure data terms in a format of 5F14.8. The fourth card contains the abscissa x = 0.0 and the appropriate pressure data at the leading edge of the annular airfoil. The fifth card contains the next abscissa and its corresponding pressure data. The abscissa value may be arbitrarily spaced in the interval [0,1] as long as the first one is 0.0 and they are strictly increasing. The second term on each card is the pressure on the outer surface of the annular airfoil. The third is the pressure on the inner surface of the annular airfoil.

If no propeller is present, i.e., a two (2) has been given as parameter 9 on the third card, the fourth and fifth terms on each card are omitted; however, if a propeller is present, i.e., a one (1) has been given as parameter 9 on the third card, then the fourth and fifth terms must be specified. The fourth term is the axial induced velocity and the fifth is the radial induced velocity. An example showing the input data for a ducted propeller is shown in Appendix A.

All cards after the first card must be repeated for each case even though some of the data may be the same.

## 3.2 OUTPUT FORMAT

The first page of output contains the input data. The second page contains the angle of attack of the annular airfoil in degrees and a table consisting of one-half the thickness and of the camber distribution from the leading edge of the foil, 0.0, to the trailing edge, 1.0, in increments of 0.05. The output obtained from the input data of the ducted propeller given in Section 3.1 is also shown in Appendix A.

If parameter 10 on the third card is a two (2), data will be punched on IBM cards by the program. The first three cards contain a total of 21 numbers, ranging from 0.0 to 1.0 in increments of 0.05, which are the abscissa values of one-half the thickness distribution. The next three cards contain the values of one-half the thickness distribution at the abscissa values given the first three cards. The next three cards, which are the abscissa values of the camber distribution, are the same as the first three cards. The last three cards contain the values of the camber distribution at the abscissa values given on the preceding three cards. All this output is punched in a format of 9F8.5.

### 3.3 FORTRAN LISTING

The FORTRAN listing of the computer program is given in Appendix B. In addition to the subroutines furnished automatically by the Bell Monitor System on the IBM 7090, the binary coding of the following subroutines available from SHARE must be added to the FORTRAN listing: BE-ELIP, AMGMHA, AMMATI, LACBRT, AQALLI, and VG-AS + C. The program takes about eight minutes to run under the Bell Monitor System.

## 4. RESULTS OF CALCULATIONS

### 4.1 ANNULAR AIRFOIL

A number of calculations were made to compare calculated duct shapes with actual shapes. Two annular airfoils from Reference 7 were considered, Duct II and the BTZ duct, and the pressure distributions for these ducts are given in Tables 1 and 2, respectively. There are two pressure distributions given for each duct; one is the experimental distribution and the other, the linearized theoretical distribution as calculated by the method of Reference 7. Tables 3 and 4 give the tabulated data for the thickness, camber, and angle of attack as calculated and the actual shape for each of the ducts. Figures 3 and 4 show a comparison of the section shapes for Duct II and the BTZ duct, respectively. The ordinates have been expanded to accentuate the differences.

A comparison of the results show that for either the linearized or experimental pressure distribution the calculated thickness is a few

TABLE 1

Pressure Distribution for Duct II

| 1 - z | Experimental | | Linearized Theory | |
|---|---|---|---|---|
| | $C_{p+}$ | $C_{p-}$ | $C_{p+}$ | $C_{p-}$ |
| Leading Edge | 1.000 | 1.000 | 1.000 | -1.000 |
| 0.0019 | 0.400 | 0.400 | 0.563 | -0.676 |
| 0.0076 | 0.151 | 0.151 | 0.117 | -0.247 |
| 0.0170 | 0.030 | 0.030 | -0.077 | -0.062 |
| 0.0302 | -0.081 | 0.058 | -0.195 | 0.051 |
| 0.0469 | -0.160 | 0.088 | -0.272 | 0.121 |
| 0.0670 | -0.199 | 0.101 | -0.319 | 0.162 |
| 0.0904 | -0.217 | 0.110 | -0.343 | 0.179 |
| 0.1170 | -0.234 | 0.112 | -0.350 | 0.178 |
| 0.1464 | -0.250 | 0.109 | -0.345 | 0.166 |
| 0.1786 | -0.275 | 0.101 | -0.334 | 0.148 |
| 0.2132 | -0.305 | 0.100 | -0.323 | 0.129 |
| 0.2500 | -0.321 | 0.107 | -0.313 | 0.114 |
| 0.2887 | -0.331 | 0.119 | -0.309 | 0.107 |
| 0.3290 | -0.338 | 0.131 | -0.311 | 0.108 |
| 0.3706 | -0.339 | 0.137 | -0.320 | 0.118 |
| 0.4132 | -0.345 | 0.135 | -0.334 | 0.134 |
| 0.4564 | -0.351 | 0.145 | -0.351 | 0.155 |
| 0.5000 | -0.355 | 0.146 | -0.367 | 0.177 |
| 0.5436 | -0.350 | 0.152 | -0.381 | 0.198 |
| 0.5868 | -0.360 | 0.159 | -0.388 | 0.215 |
| 0.6294 | -0.369 | 0.165 | -0.387 | 0.227 |
| 0.6710 | -0.359 | 0.161 | -0.376 | 0.233 |
| 0.7113 | -0.345 | 0.175 | -0.354 | 0.233 |
| 0.7500 | -0.330 | 0.171 | -0.321 | 0.230 |
| 0.7868 | -0.308 | 0.179 | -0.279 | 0.224 |
| 0.8214 | -0.270 | 0.191 | -0.229 | 0.218 |
| 0.8536 | -0.235 | 0.192 | -0.174 | 0.213 |
| 0.8830 | -0.169 | 0.192 | -0.116 | 0.209 |
| 0.9096 | -0.100 | 0.192 | -0.058 | 0.209 |
| 0.9330 | -0.032 | 0.190 | -0.002 | 0.211 |
| 0.9532 | 0.032 | 0.190 | 0.051 | 0.215 |
| 0.9698 | 0.085 | 0.192 | 0.098 | 0.220 |
| 0.9830 | 0.140 | 0.195 | 0.139 | 0.224 |
| 0.9924 | 0.160 | 0.197 | 0.170 | 0.224 |
| 0.9981 | 0.184 | 0.199 | 0.192 | 0.218 |
| 1.0000 | 0.200 | 0.200 | 1.000 | 1.000 |

TABLE 2

Pressure Distribution for the BTZ Duct

| 1 - z | Experimental | | Linearized Theory | |
|---|---|---|---|---|
| | $C_{p+}$ | $C_{p-}$ | $C_{p+}$ | $C_{p-}$ |
| Leading Edge | 1.000 | 1.000 | 1.000 | -1.000 |
| 0.0019 | 0.700 | 0.700 | -0.115 | -0.178 |
| 0.0076 | 0.120 | 0.250 | -0.120 | -0.166 |
| 0.0170 | -0.037 | 0.070 | -0.118 | -0.167 |
| 0.0302 | -0.085 | -0.025 | -0.112 | -0.170 |
| 0.0469 | -0.100 | -0.100 | -0.101 | -0.173 |
| 0.0670 | -0.110 | -0.145 | -0.103 | -0.178 |
| 0.0904 | -0.100 | -0.170 | -0.098 | -0.184 |
| 0.1170 | -0.100 | -0.182 | -0.095 | -0.190 |
| 0.1464 | -0.100 | -0.200 | -0.093 | -0.198 |
| 0.1786 | -0.100 | -0.215 | -0.093 | -0.207 |
| 0.2132 | -0.102 | -0.226 | -0.094 | -0.217 |
| 0.2500 | -0.110 | -0.241 | -0.097 | -0.228 |
| 0.2887 | -0.110 | -0.255 | -0.101 | -0.239 |
| 0.3290 | -0.110 | -0.245 | -0.105 | -0.249 |
| 0.3706 | -0.113 | -0.280 | -0.110 | -0.258 |
| 0.4132 | -0.118 | -0.280 | -0.114 | -0.256 |
| 0.4564 | -0.119 | -0.280 | -0.117 | -0.269 |
| 0.5000 | -0.112 | -0.270 | -0.119 | -0.270 |
| 0.5436 | -0.110 | -0.260 | -0.119 | -0.266 |
| 0.5868 | -0.115 | -0.250 | -0.116 | -0.258 |
| 0.6294 | -0.106 | -0.221 | -0.110 | -0.244 |
| 0.6710 | -0.090 | -0.192 | -0.100 | -0.225 |
| 0.7113 | -0.060 | -0.145 | -0.087 | -0.200 |
| 0.7500 | -0.037 | -0.110 | -0.070 | -0.169 |
| 0.7868 | -0.100 | -0.061 | -0.049 | -0.135 |
| 0.8214 | 0.011 | -0.030 | -0.025 | -0.097 |
| 0.8536 | 0.039 | -0.005 | 0.002 | -0.057 |
| 0.8830 | 0.058 | 0.020 | 0.029 | -0.017 |
| 0.9096 | 0.087 | 0.050 | 0.058 | 0.023 |
| 0.9330 | 0.062 | 0.030 | 0.086 | 0.061 |
| 0.9532 | 0.085 | 0.065 | 0.113 | 0.096 |
| 0.9698 | 0.120 | 0.100 | 0.137 | 0.126 |
| 0.9830 | 0.142 | 0.142 | 0.159 | 0.152 |
| 0.9924 | 0.164 | 0.164 | 0.176 | 0.173 |
| 0.9981 | 0.180 | 0.180 | 0.193 | 0.191 |
| 1.0000 | 1.000 | 1.000 | 1.000 | 1.000 |

TABLE 3

Section Shape for Duct II

| 1 - z | Design | | Calculated from Experimental $C_p$ | | Calculated from Theoretical $C_p$ | |
|---|---|---|---|---|---|---|
| | s(z) | c(z) | s(z) | c(z) | s(z) | c(z) |
| 0 | 0.00000 | 0.00000 | 0.0000 | 0.0000 | 0.0000 | 0.0000 |
| 0.05 | 0.02095 | 0.01085 | 0.0185 | 0.0075 | 0.0210 | 0.0125 |
| 0.10 | 0.02920 | 0.01793 | 0.0271 | 0.0140 | 0.0296 | 0.0204 |
| 0.15 | 0.03528 | 0.02348 | 0.0338 | 0.0193 | 0.0359 | 0.0254 |
| 0.20 | 0.04002 | 0.02797 | 0.0393 | 0.0240 | 0.0408 | 0.0289 |
| 0.25 | 0.04364 | 0.03162 | 0.0435 | 0.0281 | 0.0446 | 0.0315 |
| 0.30 | 0.04637 | 0.03454 | 0.0466 | 0.0314 | 0.0474 | 0.0339 |
| 0.35 | 0.04832 | 0.03681 | 0.0489 | 0.0341 | 0.0494 | 0.0362 |
| 0.40 | 0.04952 | 0.03846 | 0.0504 | 0.0360 | 0.0507 | 0.0383 |
| 0.45 | 0.05000 | 0.03952 | 0.0513 | 0.0373 | 0.0512 | 0.0400 |
| 0.50 | 0.04962 | 0.04000 | 0.0514 | 0.0379 | 0.0510 | 0.0413 |
| 0.55 | 0.04846 | 0.03988 | 0.0507 | 0.0379 | 0.0500 | 0.0418 |
| 0.60 | 0.04653 | 0.03914 | 0.0494 | 0.0374 | 0.0482 | 0.0413 |
| 0.65 | 0.04383 | 0.03774 | 0.0474 | 0.0359 | 0.0456 | 0.0396 |
| 0.70 | 0.04035 | 0.03557 | 0.0442 | 0.0336 | 0.0421 | 0.0367 |
| 0.75 | 0.03612 | 0.03248 | 0.0402 | 0.0303 | 0.0377 | 0.0325 |
| 0.80 | 0.03110 | 0.02811 | 0.0351 | 0.0260 | 0.0324 | 0.0272 |
| 0.85 | 0.02532 | 0.02170 | 0.0289 | 0.0207 | 0.0262 | 0.0209 |
| 0.90 | 0.01877 | 0.01434 | 0.0215 | 0.0141 | 0.0192 | 0.0140 |
| 0.95 | 0.01143 | 0.00685 | 0.0130 | 0.0069 | 0.0115 | 0.0069 |
| 1.00 | 0.00000 | 0.00000 | 0.0000 | 0.0000 | 0.0000 | 0.0000 |
| | $\alpha = 0$ | | $\alpha = 0.0048$ degrees | | $\alpha = -0.0720$ degrees | |

TABLE 4

Section Shape for the BTZ Duct

| 1 - z | Design | | Calculated from Experimental $C_p$ | | Calculated from Theoretical $C_p$ | |
|---|---|---|---|---|---|---|
| | s(z) | c(z) | s(z) | c(z) | s(z) | c(z) |
| 0.00 | 0.00000 | 0.00000 | 0.0000 | 0.0000 | 0.0000 | 0.0000 |
| 0.05 | 0.01257 | 0.00000 | 0.0114 | 0.0002 | 0.0129 | 0.0001 |
| 0.10 | 0.01752 | 0.00000 | 0.0172 | -0.0003 | 0.0178 | 0.0001 |
| 0.15 | 0.02119 | 0.00000 | 0.0213 | -0.0006 | 0.0214 | 0.0002 |
| 0.20 | 0.02401 | 0.00000 | 0.0245 | -0.0007 | 0.0242 | 0.0002 |
| 0.25 | 0.02618 | 0.00000 | 0.0270 | -0.0007 | 0.0265 | 0.0002 |
| 0.30 | 0.02782 | 0.00000 | 0.0288 | -0.0007 | 0.0284 | 0.0003 |
| 0.35 | 0.02899 | 0.00000 | 0.0301 | -0.0008 | 0.0298 | 0.0003 |
| 0.40 | 0.02971 | 0.00000 | 0.0309 | -0.0008 | 0.0307 | 0.0004 |
| 0.45 | 0.03000 | 0.00000 | 0.0310 | -0.0007 | 0.0311 | 0.0004 |
| 0.50 | 0.02985 | 0.00000 | 0.0304 | -0.0005 | 0.0310 | 0.0003 |
| 0.55 | 0.02925 | 0.00000 | 0.0292 | -0.0003 | 0.0302 | 0.0003 |
| 0.60 | 0.02815 | 0.00000 | 0.0273 | 0.0000 | 0.0287 | 0.0003 |
| 0.65 | 0.02611 | 0.00000 | 0.0246 | 0.0003 | 0.0266 | 0.0003 |
| 0.70 | 0.02316 | 0.00000 | 0.0211 | 0.0006 | 0.0237 | 0.0002 |
| 0.75 | 0.01953 | 0.00000 | 0.0174 | 0.0009 | 0.0202 | 0.0002 |
| 0.80 | 0.01543 | 0.00000 | 0.0134 | 0.0011 | 0.0161 | 0.0002 |
| 0.85 | 0.01107 | 0.00000 | 0.0090 | 0.0005 | 0.0116 | 0.0001 |
| 0.90 | 0.00665 | 0.00000 | 0.0052 | 0.0002 | 0.0070 | 0.0001 |
| 0.95 | 0.00262 | 0.00000 | 0.0023 | 0.0000 | 0.0027 | 0.0000 |
| 1.00 | 0.00000 | 0.00000 | 0.0000 | 0.0001 | 0.0000 | 0.0000 |
| | $\alpha = 0$ | | $\alpha = 0.0973$ degrees | | $\alpha = -0.0097$ degrees | |

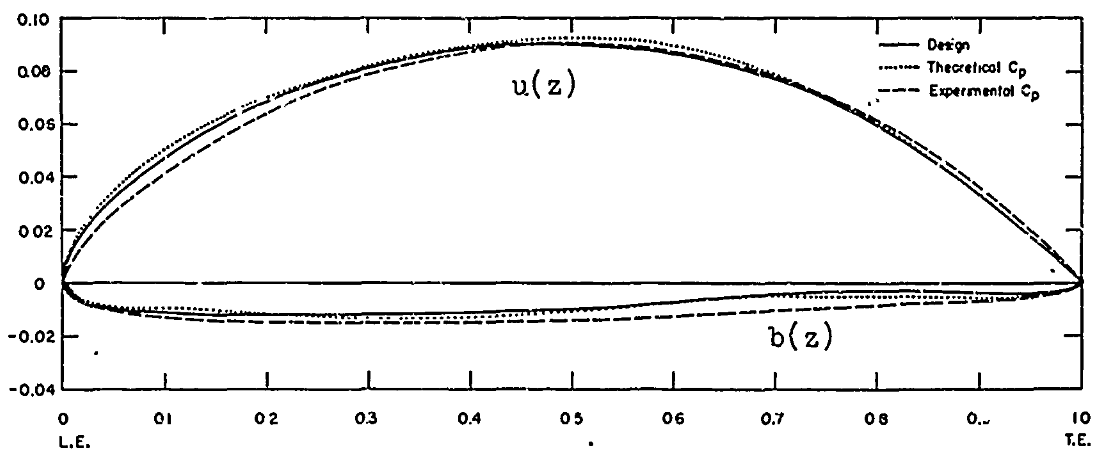


Figure 3 - Comparison of the Computed Shapes from Theoretical and Experimental Pressure Distributions with Duct II

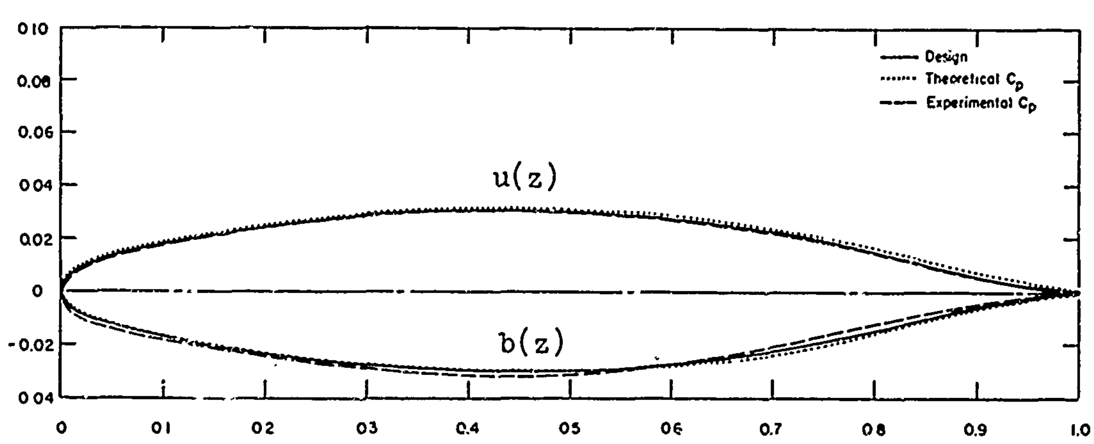


Figure 4 - Comparison of the Computed Shapes from Theoretical and Experimental Pressure Distributions with the BTZ Duct

percent larger than the design thickness. It is not possible to draw any general conclusions about the accuracy of predicting the thickness except it is reasonable and probably within the accuracy of either the linearized or experimental pressure distributions. This is all that can be expected.

The camber appears to differ by a somewhat greater magnitude than the thickness for Duct II. In fact, for the linearized pressure distribution the calculated camber is somewhat greater than the actual camber and for the experimental pressure distribution, the camber is somewhat less. The section angle of attack is less than the design angle of zero degrees for the linearized pressure distribution and slightly greater for the experimental pressure distribution. Both the camber and angle of attack show the effect of accuracy of determining the pressure distribution near the leading edge. For the linearized pressure distribution, the pressure of the duct is calculated to be infinite at the leading edge, whereas for the experimental pressure distribution the closest point measured to the leading edge was 0.025 of the chord. In either case the true pressure distribution near the leading edge is not known.

For the BTZ duct the camber and angle of attack calculated from the linearized pressure distribution are certainly within the accuracy that can be expected. The angle of attack is within 0.01 of a degree and the camber is only 1 percent of the thickness and should be considered negligible. Surprisingly, the calculated camber and angle of attack do not appear to be as accurate from the experimental pressure distribution as from the linearized. There are only two experimental points (one inside and the other outside) within 10 percent of the leading edge and both the calculated results of Reference 7 and the present calculations indicate that the point on the inside of the duct is incorrect.

The foregoing results of the ducts by themselves are presented to give an indication of the accuracy of the procedure. In reality, it makes little sense to use a linearized theory to calculate a shape from a linearized pressure distribution. The usefulness of the program presented in this report is to design a duct for a given pressure distribution when the duct is in the presence of a propeller or some other axisymmetric body. This allows a duct shape to be chosen which will not cavitate or separate.

TABLE 5

Pressure Distribution for a NACA 66-010 Thickness Distribution and Propeller Induced Velocities

| 1 - z | $c_{p+}$ | $c_{p-}$ | $(\frac{w_a}{V})p/C_T$ | $(\frac{w_a}{V})p/C_T$ |
|---|---|---|---|---|
| Leading Edge | 1.000 | 1.000 | -0.0382 | -0.0157 |
| 0.0050 | 0.104 | 0.104 | -0.0384 | -0.0158 |
| 0.0075 | 0.028 | 0.028 | -0.0386 | -0.0160 |
| 0.0125 | -0.023 | -0.023 | -0.0388 | -0.0168 |
| 0.0250 | -0.078 | -0.078 | -0.0389 | -0.0176 |
| 0.0500 | -0.125 | -0.125 | -0.0410 | -0.0180 |
| 0.0750 | -0.154 | -0.154 | -0.0426 | -0.0199 |
| 0.1000 | -0.174 | -0.174 | -0.0449 | -0.0200 |
| 0.1500 | -0.198 | -0.198 | -0.0480 | -0.0230 |
| 0.2000 | -0.215 | -0.215 | -0.0525 | -0.0280 |
| 0.2500 | -0.226 | -0.226 | -0.0564 | -0.0697 |
| 0.3000 | -0.236 | -0.236 | -0.0555 | -0.1470 |
| 0.3500 | -0.243 | -0.243 | -0.0400 | -0.1660 |
| 0.4000 | -0.249 | -0.249 | -0.0330 | -0.1760 |
| 0.4500 | -0.255 | -0.255 | -0.0210 | -0.1860 |
| 0.5000 | -0.261 | -0.261 | -0.0000 | -0.1950 |
| 0.5500 | -0.265 | -0.265 | 0.0210 | -0.1860 |
| 0.6000 | -0.270 | -0.270 | 0.0330 | -0.1760 |
| 0.6500 | -0.250 | -0.250 | 0.0400 | -0.1660 |
| 0.7000 | -0.190 | -0.190 | 0.0555 | -0.1470 |
| 0.7500 | -0.121 | -0.121 | 0.0564 | -0.0697 |
| 0.8000 | -0.052 | -0.052 | 0.0525 | -0.0280 |
| 0.8500 | 0.021 | 0.021 | 0.0480 | -0.0230 |
| 0.9000 | 0.096 | 0.096 | 0.0449 | -0.0200 |
| 0.9500 | 0.179 | 0.179 | 0.0410 | -0.0180 |
| 1.0000 | 0.271 | 0.271 | 0.0382 | -0.0157 |

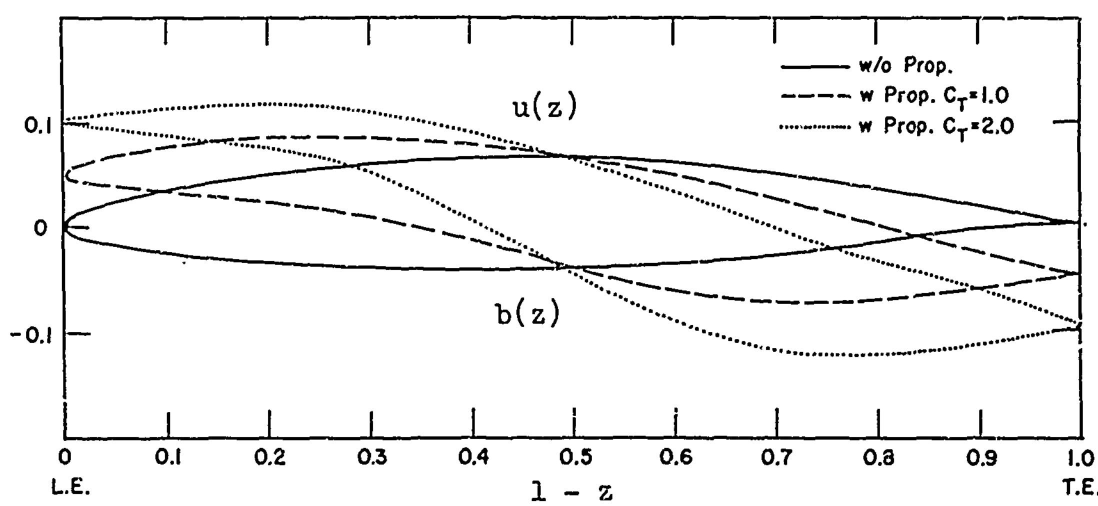


Figure 5 - Shape of Duct with Pressure Distribution Corresponding to a NACA 66-010 Thickness Form with and without a Propeller

## 4.2 DUCTED PROPELLER

The shape of the duct of a ducted propeller can be calculated by the program by inputting the steady axial and radial velocities induced by the propeller on the duct. These velocities for use in this manner are discussed in References 9 and 14 and have been tabulated in Reference 19.

Calculations for duct shape were made for a pressure distribution corresponding to the distribution on a NACA 66-010 basic thickness form,[20] Table 5. Two values of the propeller thrust loading coefficient $C_T$ were assumed, i.e., $C_T = 1.0$ and $C_T = 2.0$.

$$C_T = \frac{T}{\frac{\rho}{2} \pi R^2 V^2}$$

where

$R$ = propeller radius,

$T$ = propeller thrust,

$V$ = velocity, and

$\rho$ = mass density.

Propeller-induced velocities which were input into the program are shown in Table 5. For these calculations the tip clearance was assumed to be one percent of the propeller radius and the propeller location was assumed to be at the midchord of the duct. Also, for convenience, the thrust loading coefficient was based on the average velocity at the propeller and not the free-stream velocity as would be the usual case.

Results of these calculations are tabulated in Table 6 and plotted in Figure 5. Also plotted in this figure is the shape of the duct without the propeller. Not only is the camber and angle of attack of each duct changed considerably but the thickness is also changed. The biggest effect is on the angle of attack which goes from essentially zero to 5.35 degrees for a $C_T = 1.0$ and from zero to 10.48 degrees for a $C_T = 2.0$. Also the cambers of all the ducts are S-shaped.

With the propeller in the duct, the duct sections are thinner near the leading edge and thicker toward the trailing edge than for the duct alone. This effect increases with propeller loading. Also, the maximum duct

TABLE 6

Shape of Duct with and without a Propeller

| | Without Propeller | | With Propeller $C_T = 1.0$ | | With Propeller $C_T = 2.0$ | |
|---|---|---|---|---|---|---|
| 1 - z | s(z) | c(z) | s(z) | c(z) | s(z) | c(z) |
| 0.00 | 0.0000 | 0.0000 | 0.0000 | 0.0000 | 0.0000 | 0.0000 |
| 0.05 | 0.0192 | 0.0020 | 0.0133 | 0.0054 | 0.0073 | 0.0088 |
| 0.10 | 0.0284 | 0.0039 | 0.0203 | 0.0106 | 0.0122 | 0.0174 |
| 0.15 | 0.0352 | 0.0056 | 0.0257 | 0.0157 | 0.0163 | 0.0259 |
| 0.20 | 0.0404 | 0.0070 | 0.0302 | 0.0207 | 0.0201 | 0.0343 |
| 0.25 | 0.0445 | 0.0083 | 0.0343 | 0.0243 | 0.0240 | 0.0402 |
| 0.30 | 0.0477 | 0.0093 | 0.0382 | 0.0244 | 0.0287 | 0.0394 |
| 0.35 | 0.0500 | 0.0101 | 0.0422 | 0.0222 | 0.0344 | 0.0343 |
| 0.40 | 0.0514 | 0.0106 | 0.0457 | 0.0191 | 0.0401 | 0.0276 |
| 0.45 | 0.0521 | 0.0109 | 0.0490 | 0.0154 | 0.0460 | 0.0199 |
| 0.50 | 0.0518 | 0.0109 | 0.0519 | 0.0109 | 0.0520 | 0.0108 |
| 0.55 | 0.0507 | 0.0106 | 0.0539 | 0.0061 | 0.0571 | 0.0016 |
| 0.60 | 0.0485 | 0.0101 | 0.0542 | 0.0015 | 0.0600 | -0.0070 |
| 0.65 | 0.0445 | 0.0092 | 0.0525 | -0.0029 | 0.0604 | -0.0151 |
| 0.70 | 0.0389 | 0.0081 | 0.0485 | -0.0072 | 0.0582 | -0.0225 |
| 0.75 | 0.0322 | 0.0068 | 0.0426 | -0.0089 | 0.0529 | -0.0247 |
| 0.80 | 0.0250 | 0.0054 | 0.0353 | -0.0080 | 0.0455 | -0.0214 |
| 0.85 | 0.0177 | 0.0039 | 0.0272 | -0.0062 | 0.0368 | -0.0164 |
| 0.90 | 0.0106 | 0.0025 | 0.0188 | -0.0044 | 0.0270 | -0.0112 |
| 0.95 | 0.0044 | 0.0012 | 0.0104 | -0.0022 | 0.0164 | -0.0056 |
| 1.00 | 0.0000 | 0.0000 | 0.0000 | 0.0000 | 0.0000 | 0.0000 |
| | $\alpha$ = 0.13 degrees | | $\alpha$ = 5.35 degrees | | $\alpha$ = 10.48 degrees | |

thickness increases with propeller loading. Both effects are a consequence of assuming the propeller location to be at midchord.

If the propeller induces a velocity in the same direction as the free-stream velocity everywhere on the duct, the thickness is decreased everywhere. This would be the case when the propeller is located at or aft of the duct trailing edge. Conversely, if the propeller induces a velocity in the opposite direction to the free-stream velocity everywhere on the duct, the thickness is increased everywhere. This would be the case when the propeller is located at or forward of the duct leading edge.

The calculations for a duct shape with a propeller were based on the assumption that the inside and outside pressures were the same. Additional calculations were made for a thrust loading coefficient of two, $C_T = 2.0$, and the pressure distribution given in Table 7. The pressure distributions correspond to a NACA 66-010 thickness distribution with a NACA a = 0.8 mean line of 4-percent camber. In one case the camber is negative (toward the inside of the duct) and in the other, positive which has the effect of shifting the negative pressure from the inside to the outside of the duct.

Results of these calculations are shown in Table 8. The pressure distribution with a negative pressure on the inside of the duct results in a decrease in duct thickness whereas that with a positive pressure on the inside of the duct results in an increase in duct thickness. This is a consequence of the change in sign of $\left[\frac{w_{a(z)}}{V}\right]_{diff}$ in Equation [2.2.16]. In fact, the effect of this term is so large that the calculations show that to achieve the pressure distribution chosen for the calculation with a negative pressure inside the duct, the thickness would have to be negative near the leading edge. Since ducts of this type present construction problems, it can only be concluded that such a pressure distribution cannot be achieved for the propeller loading and location assumed.

As in Table 6, both cambers given in Table 8 are somewhat S-shaped. The difference being that for the negative pressure inside the duct, the camber is generally negative and for the positive pressure inside the duct, the camber is generally positive. It should be noted that the angle of attack varies less than a degree between the two ducts.

## TABLE 7

### Pressure Distribution of a NACA 66-010 Thickness Form with a NACA a = 0.8 Mean Line of 4 Percent Positive and Negative Camber

| 1 - z | Positive Camber | | Negative Camber | |
|---|---|---|---|---|
| | $c_{p+}$ | $c_{p-}$ | $c_{p+}$ | $c_{p-}$ |
| Leading Edge | 1.000 | 1.000 | 1.000 | 1.000 |
| 0.0050 | -0.234 | 0.387 | 0.387 | -0.234 |
| 0.0075 | -0.323 | 0.324 | 0.324 | -0.323 |
| 0.0125 | -0.378 | 0.283 | 0.283 | -0.378 |
| 0.0250 | -0.445 | 0.236 | 0.236 | -0.445 |
| 0.0500 | -0.501 | 0.195 | 0.195 | -0.501 |
| 0.0750 | -0.533 | 0.172 | 0.172 | -0.533 |
| 0.1000 | -0.558 | 0.154 | 0.154 | -0.558 |
| 0.1500 | -0.585 | 0.133 | 0.133 | -0.585 |
| 0.2000 | -0.603 | 0.120 | 0.120 | -0.603 |
| 0.2500 | -0.615 | 0.111 | 0.111 | -0.615 |
| 0.3000 | -0.628 | 0.101 | 0.101 | -0.628 |
| 0.3500 | -0.636 | 0.096 | 0.096 | -0.636 |
| 0.4000 | -0.644 | 0.090 | 0.090 | -0.644 |
| 0.4500 | -0.649 | 0.086 | 0.086 | -0.649 |
| 0.5000 | -0.656 | 0.080 | 0.080 | -0.656 |
| 0.5500 | -0.662 | 0.076 | 0.076 | -0.662 |
| 0.6000 | -0.667 | 0.073 | 0.073 | -0.667 |
| 0.6500 | -0.644 | 0.090 | 0.090 | -0.644 |
| 0.7000 | -0.575 | 0.141 | 0.141 | -0.575 |
| 0.7500 | -0.496 | 0.199 | 0.199 | -0.496 |
| 0.8000 | -0.416 | 0.257 | 0.257 | -0.416 |
| 0.8500 | -0.237 | 0.250 | 0.250 | -0.237 |
| 0.9000 | -0.067 | 0.245 | 0.245 | -0.067 |
| 0.9500 | -0.103 | 0.252 | 0.252 | -0.103 |
| 1.0000 | 1.000 | 1.000 | 1.000 | 1.000 |

## TABLE 8

### Shape of Duct with a Propeller for Positive and Negative Inside Pressures

| 1 - z | From Pressure Distribution with Positive Camber | | From Pressure Distribution with Negative Camber | |
|---|---|---|---|---|
| | s(z) | c(z) | s(z) | c(z) |
| 0.00 | 0.0000 | 0.0000 | 0.0000 | 0.0000 |
| 0.05 | 0.0292 | 0.0212 | -0.0086 | -0.0030 |
| 0.10 | 0.0428 | 0.0381 | -0.0103 | -0.0022 |
| 0.15 | 0.0532 | 0.0531 | -0.0110 | 0.0001 |
| 0.20 | 0.0619 | 0.0668 | -0.0110 | 0.0037 |
| 0.25 | 0.0697 | 0.0770 | -0.0100 | 0.0056 |
| 0.30 | 0.0774 | 0.0795 | -0.0075 | 0.0016 |
| 0.35 | 0.0853 | 0.0771 | -0.0035 | -0.0059 |
| 0.40 | 0.0924 | 0.0723 | 0.0010 | -0.0143 |
| 0.45 | 0.0991 | 0.0656 | 0.0063 | -0.0231 |
| 0.50 | 0.1054 | 0.0569 | 0.0122 | -0.0325 |
| 0.55 | 0.1100 | 0.0474 | 0.0177 | -0.0414 |
| 0.60 | 0.1118 | 0.0376 | 0.0215 | -0.0489 |
| 0.65 | 0.1104 | 0.0275 | 0.0233 | -0.0551 |
| 0.70 | 0.1056 | 0.0170 | 0.0230 | -0.0597 |
| 0.75 | 0.0972 | 0.0107 | 0.0203 | -0.0580 |
| 0.80 | 0.0857 | 0.0085 | 0.0161 | -0.0496 |
| 0.85 | 0.0717 | 0.0062 | 0.0110 | -0.0376 |
| 0.90 | 0.0561 | 0.0037 | 0.0064 | -0.0251 |
| 0.95 | 0.0378 | 0.0027 | 0.0027 | -0.0132 |
| 1.00 | 0.0000 | 0.0000 | 0.0000 | 0.0000 |
| | $\alpha$ = 11.01 degrees | | $\alpha$ = 9.95 degrees | |

## CONCLUSIONS

This report presents a computer program for the inverse problem of the annular airfoil. As a result of calculations made with this program the following conclusions can be made:

1. With the restrictions of linearized theory, duct shapes can be determined for desired pressure distributions even in the presence of a propeller.

2. For a given pressure distribution, the presence of the propeller at the duct midchord tends to increase the section angle of attack, make the camber S-shaped, and move the point of maximum thickness toward the trailing edge.

3. For a positive pressure on the inside of the duct, the duct thickness is increased. For a negative pressure on the inside of the duct and a positive pressure outside the duct thickness is decreased.

4. The propeller location and loading have important effects on the duct shape.

5. The computer program is quite versatile and will facilitate the design of ducted systems.

## ACKNOWLEDGMENTS

The authors wish to express their appreciation to personnel of the Applied Mathematics Laboratory for their assistance in programming this problem on the IBM 7090 high-speed computer. Also, the authors wish to thank Mr. E. B. Caster for the help in making computer runs and corrections in the program.

APPENDIX A - INPUT

```
   1
1 NACA 66-010 CT=1
.8          .0        40  51   26 200  45  61    1    1
.0                1.                1.                -.0382              -.0157
.005              .104              .104              -.0384              -.0158
.0075             .028              .028              -.0386              -.0160
.0125             -.023             -.023             -.0388              -.0168
.025              -.078             -.078             -.0389              -.0176
.05               -.125             -.125             -.041               -.018
.075              -.154             -.154             -.0426              -.0199
.10               -.174             -.174             -.0449              -.02
.15               -.198             -.198             -.048               -.023
.20               -.215             -.215             -.0525              -.028
.25               -.226             -.226             -.0564              -.0697
.3                -.236             -.236             -.0555              -.147
.35               -.243             -.243             -.04                -.166
.4                -.249             -.249             -.033               -.176
.45               -.255             -.255             -.021               -.186
.50               -.261             -.261             .0                  -.195
.55               -.265             -.265             .021                -.186
.6                -.27              -.27              .033                -.176
.65               -.25              -.25              .04                 -.166
.7                -.19              -.19              .0555               -.147
.75               -.121             -.121             .0564               -.0697
.8                -.052             -.052             .0525               -.028
.85               .021              .021              .048                -.023
.90               .096              .096              .0449               -.02
.95               .179              .179              .041                -.018
1.                .271              .271              .0382               -.0157
```

APPENDIX A - Continued

OUTPUT

NACA 66010 CT=1

CALCULATION OF THE THICKNESS DISTRIBUTION AND THE CAMBER DISTRIBUTION USING THE FOLLOWING DATA.

| CHORD DIAMETER RATIO | WAKE FRACTION |
|---|---|
| 0.80000000 | 1.00000000 |

| ABSCISSA OF THE PRESSURE DISTRIBUTION | OUTER PRESSURE | INNER PRESSURE | INDUCED VELOCITY TERMS AXIAL | RADIAL |
|---|---|---|---|---|
| -0. | 1.0000000 | 1.0000000 | -0.0382000 | -0.0157000 |
| 0.00500 | 0.1040000 | 0.1040000 | -0.0384000 | -0.0158000 |
| 0.00750 | 0.0280000 | 0.0280000 | -0.0386000 | -0.0160000 |
| 0.01250 | -0.0230000 | -0.0230000 | -0.0388000 | -0.0163000 |
| 0.02500 | -0.0780000 | -0.0780000 | -0.0389000 | -0.0176000 |
| 0.05000 | -0.1250000 | -0.1250000 | -0.0410000 | -0.0180000 |
| 0.07500 | -0.1540000 | -0.1540000 | -0.0426000 | -0.0199000 |
| 0.10000 | -0.1740000 | -0.1740000 | -0.0449000 | -0.0200000 |
| 0.15000 | -0.1980000 | -0.1980000 | -0.0480000 | -0.0230000 |
| 0.20000 | -0.2150000 | -0.2150000 | -0.0525000 | -0.0280000 |
| 0.25000 | -0.2260000 | -0.2260000 | -0.0564000 | -0.0697000 |
| 0.30000 | -0.2360000 | -0.2360000 | -0.0555000 | -0.1470000 |
| 0.35000 | -0.2430000 | -0.2430000 | -0.0400000 | -0.1660000 |
| 0.40000 | -0.2490000 | -0.2490000 | -0.0330000 | -0.1760000 |
| 0.45000 | -0.2550000 | -0.2550000 | -0.0210000 | -0.1860000 |
| 0.50000 | -0.2610000 | -0.2610000 | -0. | -0.1950000 |
| 0.55000 | -0.2650000 | -0.2650000 | 0.0210000 | -0.1860000 |
| 0.60000 | -0.2700000 | -0.2700000 | 0.0330000 | -0.1760000 |
| 0.65000 | -0.2500000 | -0.2500000 | 0.0400000 | -0.1660000 |
| 0.70000 | -0.1900000 | -0.1900000 | 0.0555000 | -0.1470000 |
| 0.75000 | -0.1210000 | -0.1210000 | 0.0564000 | -0.0697000 |
| 0.80000 | -0.0520000 | -0.0520000 | 0.0525000 | -0.0280000 |
| 0.85000 | 0.0210000 | 0.0210000 | 0.0480000 | -0.0230000 |
| 0.90000 | 0.0960000 | 0.0960000 | 0.0449000 | -0.0200000 |
| 0.95000 | 0.1790000 | 0.1790000 | 0.0410000 | -0.0180000 |
| 1.00000 | 0.2710000 | 0.2710000 | 0.0382000 | -0.0157000 |

APPENDIX A - Continued

OUTPUT

THE FOLLOWING TABLE IS THE DISTRIBUTION OF THE DESIRED FOIL
AT A 5.34884 DEGREE ANGLE OF ATTACK.

| ABSCISSA | THICKNESS | CAMBER |
|---|---|---|
| LEADING EDGE | 0. | 0. |
| 0.05 | 0.013274 | 0.005393 |
| 0.10 | 0.020276 | 0.010640 |
| 0.15 | 0.025718 | 0.015720 |
| 0.20 | 0.030249 | 0.020667 |
| 0.25 | 0.034266 | 0.024266 |
| 0.30 | 0.038213 | 0.024375 |
| 0.35 | 0.042190 | 0.022269 |
| 0.40 | 0.045733 | 0.019137 |
| 0.45 | 0.049012 | 0.015378 |
| 0.50 | 0.051928 | 0.010850 |
| 0.55 | 0.053906 | 0.006127 |
| 0.60 | 0.054231 | 0.001526 |
| 0.65 | 0.052461 | -0.002947 |
| 0.70 | 0.048536 | -0.007205 |
| 0.75 | 0.042579 | -0.008922 |
| 0.80 | 0.035285 | -0.008012 |
| 0.85 | 0.027224 | -0.006227 |
| 0.90 | 0.018823 | -0.004351 |
| 0.95 | 0.010426 | -0.002209 |
| TRAILING EDGE | 0.000053 | -0.000003 |

## APPENDIX B - FORTRAN LISTING OF COMPUTER PROGRAM

```
      FOR
      DIMENSION POUT(37),PIN(37),PAX(37),PRAD(37),THETA(37),THETAB(101)
     1,THICK(101),OMEGA(37 ),CPRIME(101) ,C(21),S(21),Z(21),X(37)
     2,DUM(21)
      READ 199,NCASE
  199 FORMAT (I4)
      DO 198 ICASE = 1,NCASE
      READ 99
   99 FORMAT (72H1
     1
      READ 10, H,WXD,M,N,NZ,NP,NH,IJK,J1,IPUN
   10 FORMAT (2F10.6,8I4)
      READ 11, (X(I),POUT(I),PIN(I),PAX(I),PRAD(I), I=1,NZ)
   11 FORMAT (5F14.8)
      WAKE = 1.0 - WXD
      PRINT 99
      PRINT 13, H,WAKE
   13 FORMAT (98H0 CALCULATION OF THE THICKNESS DISTRIBUTION AND THE CAM
     1BER DISTRIBUTION USING THE FOLLOWING DATA.  //22H CHORD DIAMETER R
     2ATIO  5X,15H WAKE FRACTION  /7X,F12.8,9X,F12.8//17H ABSCISSA OF TH
     3E 10X,16H OUTER PRESSURE 5X,16H INNER PRESSURE 10X,24H INDUCED VEL
     4OCITY TERMS  /23H PRESSURE DISTRIBUTION 52X,7H AXIAL 6X,8H RADIAL
     5  //)
      PRINT 14, (X    (I),POUT(I),PIN(I),PAX(I),PRAD(I),I=1,NZ)
   14 FORMAT  (1H 8X,F8.5,14X,F12.7,9X,F12.7,12X,F12.7,F14.7)
      DO 765 I=1,N
  765 PRAD(I) = -PRAD(I)
      PI = 3.14159265
      DN = N-1
      DELTA = PI/DN
      NJN = N-3
      DO 115 I=1,NZ
      X(I) = 1.0 - X(I)
      XARG = 2.0*X(I) - 1.0
      THETA(I) = ACOSF(ABSF(XARG))
      IF (XARG) 114,115,115
  114 THETA(I) = PI - THETA(I)
  115 CONTINUE
      THETAB(1) = 0.0
      DO 116 I=2,N
  116 THETAB(I) = THETAB(I-1) + DELTA
   18 IF (ABSF(POUT(1) -PIN(1)) - .0001) 210,210,211
  210 IZ = 1
      GO TO 212
  211 IZ = 2
  212 DO 25 I=IZ,NZ
      OMEGA(I) = PI*(.25*(POUT(I) + PIN(I)) - PAX (I))
   25 PAX (I) = .5*(POUT(I) - PIN(I))*SINF(THETA(I))
C PAX IS NOW THE VELOCITY DIFFERENCE TERM TIMES SINE( THETA ).
      GO TO (27 ,225),IZ
  225 OMEGA(1) = -PI*PAX(1)
      DO 224 I=IZ,NZ
      THETA(I-1) = THETA(I)
  224 PAX(I-1) = PAX(I)
      NZ1 = NZ-1
      CALL DISCOT (0.0,0.0,THETA,PAX,PAX,-020,NZ1,0,PAXT)
      DO 231 I=1,NZ
      POUT(I) = THETA(I)
  231 PIN(I) = PAX(I)
      DO 230 I=2,NZ
```

```
      THETA(I) = POUT (I-1)
  230 PAX(I) = PIN(I-1)
      THETA(1) = 0.0
      PAX(1) = PAXT
   27 Z(1) = 0.0
      DO 30 I=2,21
   30 Z(I) = Z(I-1) + .05
      CALL THKDIS (DELTA,DN,                    H,M,N,NJN,NZ,PI,THICK,  YV18 230
     1PAX,OMEGA,NP,NH          ,THETA,THETAB,Z,S,IJK)
      CALL CAMBER (DELTA,DN, H, N,NJN,NZ,PI,THICK,WAKE,PAX,PRAD,J1,THETA
     1B,THETA,ATTACK,CPRIME,S,Z)
      CALL SOLVE (IJK,PI,THETAB,CPRIME,N,Z,C)
      PRINT 98, ATTACK
   98 FORMAT (67H1 THE FOLLOWING TABLE IS THE DISTRIBUTION OF THE DESIRE
     1D FOIL AT A  F9.5,25H DEGREE ANGLE OF ATTACK.   /15X,9H ABSCISSA 1
     20X,10H THICKNESS 8X,8H CAMBER  //)
      PRINT 150, S(21),C(21)
  150 FORMAT (11X,14H LEADING EDGE 9X,F10.6,F16.6)
      DO 777 I=2,20
      JIP = 22-I
  777 PRINT 97, Z(I),S(JIP),C(JIP)
   97 FORMAT (10X,F12.2,12X,F10.6,F16.6)
      PRINT 151,S(1),C(1)
  151 FORMAT(10X,15H TRAILING EDGE 9X,F10.6,F16.6)
      IF (IPUN - 1) 198,198,599
  599 PUNCH 600, (Z(I),I=1,21)
      DO 610 I=1,21
      JIP = 22- I
  610 DUM(I) = C(JIP)
      PUNCH 600, (DUM(I),I=1,21)
      DO 611 I=1,21
      JIP = 22- I
  611 DUM(I) = S(JIP)
      PUNCH 600, (Z(I),I=1,21)
      PUNCH 600, (DUM(I),I=1,21)
  600 FORMAT (9F8.5)
  198 CONTINUE
      CALL ENDJOB                                                       YV18 310
      END                                                               YV18 320
       FOR                                                              YV181010
      SUBROUTINE THKDIS (DELTA,DN,H,M,N,NJN,NZ,PI,THICK,PAX,OMEGA,NP,NH
     1,THETA,THETAB,Z,S,IJK)
      DIMENSION ALPHA(40,40),B(40,101),GAMMA(40,40),FM(40),FTHETB(101),
     1OMEGA(37),THETAB(101),THICK(101),PAX(37),THETA(37)
      EQUIVALENCE                     (GAMMA,ALPHA)
      ERROR = 0.00001
      CALL KERNEL (B,DELTA,H,M,                   N,PI,ERROR,KEEP)      YV070250
C LOOP FOR CALCULATING A SERIES OF F(THETA BAR) VALUES BY INCREMENTING  YV070260
C THETA BAR FROM 0.0 TO PI.                                             YV070270
      DO 52 I=1,N
      IF (I-1) 52,52,51                                                 YV070290
   51 IF(I-N)54,52,52                                                   YV070315
   54 SINB = 1.0/(2.0*PI*SINF(THETAB(I)))                               YV070330
   52 CALL USEGM (THETAB(I),SINB,I,PI,NP,N,DN,H,THETA,PAX,NZ,OMEGA,NH,
     1FTHETB(I))
      CALL CALCAL (ALPHA,B,DELTA,         KEEP,N,THETAB,PI             )YV070430
      CALL CALCFM (B,DELTA,FM,FTHETB,         KEEP,N                )   YV070440
C LOOPS FOR PREPARATION OF COEFFICIENTS OF LINEAR SYSTEM FOR MATINV     YV070520
   61 DO 70 I=1,KEEP                                                    YV070530
      DO 70 J=1,KEEP                                                    YV070530
```

```
      IF (I-J) 71,72,71
   72 GAMMA(I,J) = 1.0 - ALPHA(I,J)/PI                                  YV070540
      GO TO 70
   71 GAMMA(I,J) = -ALPHA(I,J)/PI                                       YV070560
   70 CONTINUE
      CALL MATINV (GAMMA,KEEP,FM,1,X,ID)                                YV070570
      IF(2-ID) 75,76,75
   76 PRINT 77                                                          YV070590
   77 FORMAT (117HOCOEFFICIENT MATRIX IS SINGULAR.  THE INTEGRAL EQUATIOYV070600
     1N IS EITHER INSOLVABLE OR HAS AN INFINITE NUMBER OF SOLUTIONS.  ) YV070610
      CALL ENDJOB
C LOOPS FOR CALCULATION OF THE SLOPE OF THE THICKNESS DISTRIBUTION.     YV070700
   75 DO 90 I=1,N
      IF (I-1) 92,92,85
   85 IF(I-N) 86,93,93
   92 THICK (I) = FTHETC(I) + FM(1)/PI
      DO 150 J = 2,KEEP
      DJ = J
  150 THICK (I) = THICK (I) + FM(J)*DJ/PI
      GO TO 90
   93 THICK (I) = FTHETB(I) + FM(1)/PI
      DO 149 J = 2,KEEP
      DJ = J
  149 THICK (I) = THICK (I) - (-1.0)** J*FM(J)*DJ/PI
      GO TO 90
   86 SINT= SINF(THETAB(I))                                             YV070720
      SUM = FM(1)                                                       YV070730
      DO 91 J=2,KEEP                                                    YV070740
      DJ = J                                                            YV070750
   91 SUM = SUM + FM(J)*SINF(DJ*THETAB(I))/SINT                         YV070760
      THICK (I) = FTHETB(I) + SUM/PI
   90 CONTINUE
      CALL SOLVE (IJK,PI,THETAB,THICK ,N,Z,S)
      RETURN                                                            YV181080
      END                                                               YV181090
       FOR                                                              YV14  10
      SUBROUTINE KERNEL (B,DELTA,H,M,N,PI,ERROR,KEEP)
      DIMENSION B(40,101),CONSK(101),EE(101),FB(101),THETA1(101),       YV140030
     1THETA5(201),FBCOS(201)                                            YV140040
C LOOP FOR VARYING THETA 1 IN CALCULATION OF FOURIER COEFFICIENTS FOR   YV140050
C APPROXIMATION OF THE KERNEL.                                          YV140060
      KEEP = 1
      DO 200 I=1,N                                                      YV140070
      IN = 1                                                            YV140080
C LOOP FOR CALCULATION OF ACTUAL FOURIER COEFFICIENTS -- B(THETA 1).    YV140090
      DO 202 L=1,M                                                      YV140100
      DL = L                                                            YV140110
      II = 1                                                            YV140120
      IF (I-1) 700,700,710                                              YV140130
  700 THETA1(1) = 0.0                                                   YV140140
C THETA1 VARIES FROM 0.0 TO PI,                                         YV140150
      GO TO 755                                                         YV140160
  710 THETA1(I) = THETA1(I-1) + DELTA                                   YV140170
  755 COS1 = COSF(THETA1(I))                                            YV140180
      IF (10-L) 740,741,741                                             YV140190
  741 GO TO (745,760),IN                                                YV140200
  745 IN = 2                                                            YV140210
      NN = 51                                                           YV140220
      NNN = 51                                                          YV140230
      ANGLE  = PI/50.0                                                  YV140240
```

```
      FIRST = 0.0                                                       YV140250
      JJJ = 1                                                           YV140260
      GO TO 750                                                         YV140280
  740 IF (20-L) 742,743,743                                             YV140290
  743 GO TO (746,746,760),IN                                            YV140300
  746 IN = 3                                                            YV140310
      DO 201 J=1,50                                                     YV140320
      LESS = 103 - 2*J                                                  YV14 325
      MINUS = 52-J                                                      YV14 326
      THETA5(LESS) = THETA5(MINUS)                                      YV140330
  201 FB(LESS) = FB(MINUS)                                              YV140340
      NN = 100                                                          YV140350
      NNN = 101                                                         YV140360
      ANGLE = PI/100.0                                                  YV140370
      FIRST = ANGLE                                                     YV140380
      JJJ = 2                                                           YV140400
      GO TO 750                                                         YV140410
  742 GO TO (747,747,747,760),IN                                        YV140420
  747 IN = 4                                                            YV140430
      DO 205 J=1,100                                                    YV140440
      LESS = 203 - 2*J                                                  YV14 445
      MINUS = 102 - J                                                   YV14 446
      THETA5(LESS) = THETA5(MINUS)                                      YV140450
  205 FB(LESS) = FB(MINUS)                                              YV140460
      NN = 200                                                          YV140470
      NNN = 201                                                         YV140480
      ANGLE = PI/200.0                                                  YV140490
      FIRST = ANGLE                                                     YV140500
      JJJ = 2                                                           YV140520
  750 CALL INTGRL (ANGLE ,CONSK,COS1,EE,FB,FIRST,I,II,L,      NN,NNN,   YV140530
     1THETA1(I),THETA5,JJJ,M,H)
  760 DO 203 J=1,NNN                                                    YV140560
  203 FBCOS(J) = FB(J)*COSF(DL*THETA5(J))                               YV140570
C INTEGRAND VALUES FOR INTEGRATION WITH RESPECT TO THETA5               YV140580
      SUMB = FBCOS(1) + 4.0*FBCOS(NNN-1) + FBCOS(NNN)                   YV140590
      NJN = NNN-3                                                       YV140600
      DO 204 J=2,NJN,2                                                  YV140610
  204 SUMB = SUMB + 4.0*FBCOS(J) + 2.0*FBCOS(J+1)                       YV140620
      B(L,I) = 2.0*ANGLE*SUMB/(3.0*PI)                                  YV140670
C B IS THE VALUE OF THE FOURIER COEFFICIENT FOR EACH VALUE OF THETA 1.  YV140680
      IF (ABSF(B(L,I)) - ERROR) 790,790,202                             YV140690
C CHECK FOR THE CONVERGENCE OF THE FOURIER COEFFICIENTS                 YV140700
  202 CONTINUE                                                          YV140710
      KEEP = M
      GO TO 200                                                         YV140770
  790 L = L+1
      DO 771 LL=L,M                                                     YV140840
  771 B(LL,I) = 0.0                                                     YV140850
      KEEP1 = L - 1
      IF (KEEP - KEEP1) 795,200,200
  795 KEEP = KEEP1
  200 CONTINUE                                                          YV140860
      RETURN                                                            YV140870
      END                                                               YV140880
       FOR
      SUBROUTINE USEGM (THETAB,SINB,I,PI,NP,N,DN,H,THETA,WDIFFR,NZ,OMEGA
     1,NH,SUM)
      DIMENSION THETA4(101),       WDIFFR(37 ),OMEGA(37 ),ANSWER(101),  YV21 030
     1T(101),F(101),R(507),A(100),THETA(37)                             YV21 040
      IF (I-1) 501,501,500                                              YV21 050
```

```
  501 LIFT = 1                                                          YV21 060
      NP1 = NP/2
      NP2 = NP1 + 1
      P = NP1                                                           YV21 070
      DELANG = PI/P                                                     YV21 080
      THETA4(1) = 0.0                                                   YV21 090
      ANSWER(1) = 0.0                                                   YV21 100
C LOOP FOR CALCULATING SERIES OF FUNCTIONAL VALUES FOR HARMONIC ANALYSISYV21 110
      DO 510 J = 2,NP2                                                  YV21 120
      THETA4(J) = THETA4(J-1) + DELANG                                  YV21 130
      TLOW = -CUBERTF(PI - THETA4(J))                                   YV21 140
      TUP = CUBERTF(THETA4(J))                                          YV21 150
      DELTAT = (TUP - TLOW)/DN                                          YV21 160
      SIN2 = SINF(THETA4(J))**2                                         YV21 170
C LOOP FOR EVALUATION OF INTEGRATION WITH RESPECT TO T.                 YV21 180
      DO 515 K=1,N                                                      YV21 190
      IF (K-1) 516,516,517                                              YV21 200
  516 T(1) = TLOW                                                       YV21 210
      GO TO 555                                                         YV21 220
  517 T(K) = T(K-1) + DELTAT                                            YV21 230
  555 IF (ABSF(T(K)) - 0.0001) 556,556,557                              YV21 240
  556 F(K) = 0.0                                                        YV21 250
      GO TO 515                                                         YV21 260
  557 X = THETA4(J) - T(K)**3                                           YV21 270
      COST = COSF(THETA4(J))                                            YV21 280
      COSX = COSF(X)                                                    YV21 290
C CALCULATION OF ELLIPTIC CONSTANT K                                    YV21 300
      CONK = SQRTF(1.0/(.25*(H*(COST - COSX))**2 + 1.0))                YV21 310
C SUBROUTINE FOR CALCULATION OF ELLIPTIC INTEGRALS.                     YV21 320
      CALL WORK (CONK,THETA4(J),T(K),H,EK,EE,DIF)                       YV21 330
C SUBROUTINE FOR INTERPOLATION OF VELOCITY DIFFERENCE VALUES.           YV21 350
      CALL DISCOT (X,X,THETA,WDIFFR,WDIFFR,-120,NZ,0,WDIFR)
C CALCULATION OF INTEGRAND VALUES FOR INTEGRATION WITH RESPECT TO T.    YV21 370
      F(K) = H*WDIFR*CONK*DIF*3.0*T(K)**2        /4.0                   85
  515 CONTINUE                                                          YV21 390
      SUMT = F(1) + 4.0*F(N-1) + F(N)                                   YV21 400
      NTN = N-3                                                         YV21 410
      DO 560 L=2,NTN,2                                                  YV21 420
  560 SUMT = SUMT + 4.0*F(L) + 2.0*F(L+1)                               YV21 430
C SUBROUTINE FOR INTERPOLATION OF MEAN VELOCITY MINUS AVERAGE INDUCED   YV21 450
C                   VELOCITY VALUES                                     YV21 460
      CALL DISCOT (THETA4(J),THETA4(J),THETA,OMEGA,OMEGA,-120,NZ,0,
     1ZOMEGA)
  510 ANSWER(J) = (DELTAT*SUMT/3.0 + ZOMEGA)*SIN2                       YV21 480
      DO 520 J=2,NP1
      NMINUS = NP - J + 2
  520 ANSWER(NMINUS) = ANSWER(J)
C SUBROUTINE FOR CALCULATING FOURIER COEFFICIENTS.                      YV21 530
      CALL GMHAS (NP,NH,ANSWER,R(507))                                  YV21 540
      MAX = 507                                                         YV21 550
      DO 580 L=1,NH                                                     YV21 560
      IL = MAX-5*L                                                      YV21 570
  580 A(L) = R(IL)                                                      YV21 580
  500 SUM = A(1)/(2.0*PI)                                               YV21 630
      LEFT=LIFT
      GO TO (570,571),LEFT                                              YV21 640
  570 DO 572 L=2,NH                                                     YV21 650
      DL = L                                                            YV21 660
  572 SUM = SUM + DL*A(L)/(2.0*PI)                                      YV21 670
      LIFT = 2                                                          YV21 680
```

```
      GO TO 599
  571 IF (I-N) 575,574,574                                              YV21 700
  575 DO 576 L=2,NH                                                     YV21 710
      DL = L                                                            YV21 720
  576 SUM = SUM + A(L)*SINF(DL*THETAB)*SINB                             YV21 730
      GO TO 599                                                         YV21 740
  574 DO 577 L=2,NH                                                     YV21 750
      DL = L                                                            YV21 760
  577 SUM = SUM - (-1.0)**L*DL*A(L)/(2.0*PI)                            YV21 770
  599 RETURN                                                            YV21 780
      END                                                               YV21 790
       FOR                                                              YV070010
      SUBROUTINE CALCAL(ALPHA,B,DELTA,       KEEP,N,THETA1,PI           YV070020
      DIMENSION ALPHA(40,40),B(40,101),THETA1(101)                      YV070030
      NN=(N-3)/2                                                        YV070040
      DO 352 LL=1,KEEP
      DO 350 L=1,KEEP                                                   YV070100
      DL=L                                                              YV070110
      SUMAL = B(LL,1)*DL + 4.0*B(LL,N-1)*SINF(DL*THETA1(N-1))/SINF(THETAYV070120
     11(N-1))- B(LL,N)*DL*COSF(DL*PI)
      DO 351 J=1,NN                                                     YV070150
  351 SUMAL = SUMAL + 4.0*B(LL,2*J)*SINF(DL*THETA1(2*J))/SINF(THETA1(2*JYV070160
     1)) + 2.0*B(LL,2*J+1)*SINF(DL*THETA1(2*J+1))/SINF(THETA1(2*J+1))   YV070170
  350 ALPHA(LL,L) = DELTA*SUMAL/3.0                                     YV070180
  352 CONTINUE                                                          YV070260
      RETURN                                                            YV070270
      END                                                               YV070280
       FOR                                                              YV070010
      SUBROUTINE CALCFM(B,DELTA,FM,FTHET1,       KEEP,N                 YV07
      DIMENSION B(40,101),FM(40),FTHET1(101)                            YV070030
      NN=(N-3)/2                                                        YV070040
      DO 301 L=1,KEEP                                                   YV070050
      SUMFM=B(L,1)*FTHET1(1)+4.0*B(L,N-1)*FTHET1(N-1)+B(L,N)*FTHET1(N)  YV070100
      DO 300 I=1,NN
  300 SUMFM=SUMFM+4.0*B(L,2*I)*FTHET1(2*I)+2.0*B(L,2*I+1)*FTHET1(2*I+1) YV070120
  301 FM(L) = DELTA*SUMFM/3.0                                           YV070130
      RETURN
      END                                                               YV070210
       FOR
      SUBROUTINE CHEAT (THETA4,T,H,DIF)                                 YV07 010
      CON = H*(T**6/2.0*COSF(THETA4) - T**3*SINF(THETA4))               YV07 020
      CK = CON/SQRTF(4.0+CON**2)                                        YV07 030
      IF (CK) 930,931,930                                               YV07 040
  930 ALAM = LOGF(ABSF(4.0/CK))                                         YV07 050
      DIF = ALAM - 1.0 - ALAM*CK**2/4.0                                 YV07 060
      RETURN                                                            YV07 070
  931 DIF = 0.0                                                         YV07 080
      RETURN                                                            YV07 090
      END                                                               YV07 100
       FOR                                                              YV07 005
      SUBROUTINE WORK (CONK,THETA4,T,H,EK,EE,DIF)                       YV07 010
      IF (CONK - 0.995) 940,940,941                                     YV07 020
  940 CALL ELLIP (0.0,CONK,?,ZZ,EK,EE)                                  YV07 030
      GO TO 981                                                         YV07 040
  941 IF (CONK - 0.999999)      ,942,943                                YV07 050
  942 CALL VELLIP (CONK,EE,EK)                                          YV07 060
  981 DIF = EK - EE                                                     YV07 070
      RETURN                                                            YV07 080
  943 CALL CHEAT (THETA4,T,H,DIF)                                       YV07 090
      EK = DIF + 1.0                                                    YV07 100
```

```
      EE = -1.0                                                         YV07 110
  945 RETURN                                                            YV07 120
      END                                                               YV07 130
       FOR                                                              YV07 010
      SUBROUTINE EELLIP (CONSK,EE)                                      YV07 020
      IF (CONSK - 0.995) 940,940,941                                    YV07 030
  940 CALL  ELLIP (0.0,CONSK,Z,ZZ,ZZZ,EE)                               YV07 040
      RETURN                                                            YV07 050
  941 YK = 1.0 - CONSK**2                                               YV07 060
      IF (YK) 942,942,943                                               YV07 070
  943 ALAM = LOGF(4.0/SQRTF(YK))                                        YV07 080
      EE = 1.0+(2.0*ALAM-1.0)*YK/4.0 + 3.0*(ALAM-13.0/12.0)*YK**2/16.0  YV07 090
      RETURN                                                            YV07 100
  942 EE = 1.0                                                          YV07 110
      RETURN                                                            YV07 120
      END                                                               YV07 130
       LOAD BATCH
       FOR
      SUBROUTINE VELLIP  (XK,EE,EK)                                     YV01  10
C EVALUATION OF COMPLETE ELLIPTIC INTEGRALS WHEN K SQUARED IS GREATER   YV01  20
C THAN .99 BUT NOT EQUAL TO 1.0 BY ASYMPTOTIC SERIES.                   YV01  30
      YK = 1.0 - XK**2                                                  YV01  40
      ALAM = LOGF(4.0/SQRTF(YK))                                        YV01  50
      EE = 1.0 + (2.0*ALAM-1.0)*YK/4.0 + 3.0*(ALAM-13.0/12.0)*YK**2/16.0YV01  60
      EK = ALAM + (ALAM-1.0)*YK/4.0 + 9.0*(ALAM-7.0/6.0)*YK**2/64.0     YV01  70
      RETURN                                                            YV01  80
      END                                                               YV01  90
       FOR                                                              YV33
      SUBROUTINE SOLVE(JK,PI,THETAB,F,N,Z,STORE)                        YV33
      DIMENSION THETAB(101),F(101),STORE(21),Z(21)                      YV33
      IJK=JK                                                            YV33
      DO 101 I=1,20                                                     YV33
      DIJK=IJK-1                                                        YV33
      ZARG=2.0*Z(I)-1.0                                                 YV33
      ANG=ACOSF(ABSF(ZARG))                                             YV33
      IF(ZARG)134,135,135                                               YV33
  134 ANG=PI-ANG                                                        YV33
  135 DEL=ANG/DIJK                                                      YV33
      CALL DISCOT(DEL,DEL,THETAB,F,F,-120,N,0,RESULT)                   YV33
      STORE(I)=F(1)+4.0*RESULT                                          YV33
      IJK=IJK-1                                                         YV33
      DO 100 J=3,IJK,2                                                  YV33
      DJ=J-1                                                            YV33
      T=DJ*DEL                                                          YV33
      CALL DISCOT(T,T,THETAB,F,F,-120,N,0,RESULT)                       YV33
      STORE(I)=STORE(I)+2.0*RESULT                                      YV33
      T=(DJ+1.0)*DEL                                                    YV33
      CALL DISCOT(T,T,THETAB,F,F,-120,N,0,RESULT)                       YV33
  100 STORE(I)=STORE(I)+4.0*RESULT                                      YV33
      CALL DISCOT(ANG,ANG,THETAB,F,F,-120,N,0,RESULT)
      STORE(I)=(STORE(I)+RESULT)*DEL/3.0                                YV33
  101 IJK=IJK-1                                                         YV33
      STORE(21)=0.0                                                     YV33
      RETURN                                                            YV33
      END                                                               YV33
       FOR                                                              YV18D 10
      SUBROUTINE CWORK (CONK,TERM,EK,EE,DIF)                            YV18D 20
      IF (CONK - 0.995) 940,940,941                                     YV18D 30
  940 CALL ELLIP (0.0,CONK,ZZ,ZZZ,EK,EE)                                YV18D 40
      GO TO 981                                                         YV18D 50
```

```
941 IF (CONK - 0.999999) 942,942,943                                    YV18D 60
942 CALL VELLIP (CONK,EE,EK)                                            YV18D 70
981 DIF = EK - EE                                                       YV18D 80
    RETURN                                                              YV18D 90
943 IF (TERM) 944,945,944                                               YV18D100
945 DIF = 1.0                                                           YV18D110
    GO TO 946                                                           YV18D120
944 TERM2 = TERM**2                                                     YV18D130
    ALAM = LOGF(ABSF(4.0*SQRTF(TERM2 + 1.0)/TERM))                      YV18D140
    DIF = ALAM - 1.0 - ALAM*TERM2/(4.0*(TERM2 + 1.0))                   YV18D150
946 EK = DIF + 1.0                                                      YV18D160
    EE = -1.0                                                           YV18D170
    RETURN                                                              YV18D180
    END                                                                 YV18D190
     FOR                                                                YV18F 10
     FOR                                                                YV320010
    SUBROUTINE CAMBER (DELTA,DN,H,N,NJN,NZ,PI,THICK,WAKE,WDIFFR,PRAD    YV320020
   1,J1,THETAB,THETA,ATTACK,CPRIME,S,Z)
    DIMENSION THICK(101),WDIFFR(37),PRAD(37),THETAB(101),THETA(37),     YV320040
   1CPRIME(101),CINT1(101),CINT2(101),CINT3(101),         VDIFR(101) ,  YV320050
   2S(21),Z(21)
    N1 = N-1                                                            YV320080
    RADIAL = 0.0                                                        YV320090
    DO 50 I=2,N1                                                        YV320100
    CALL INTRL1 (CINT1(I),DELTA,H,                 NJN,NZ,PI,WAKE       YV320110
   1,WDIFFR,THETA,N,THETAB,VDIFR,I)                                     YV320120
    CALL MUSK (DELTA,THETA,WDIFFR,NZ,N,H,NJN,CINT3(I),THETAB,
   1          I,WAKE,PI,VDIFR)                                          YV320140
    CALL INTRL2 (N1,I,THETAB,H,Z,S,DELTA,THICK,NJN,N,CINT2(I),PI)
    GO TO (48,50),J1                                                    YV320170
 48 CALL DISCOT (THETAB(I),THETAB(I),THETA,PRAD,PRAD,-120,NZ,0,RADIAL)YV320180
 50 CPRIME(I-1) =   (CINT1(I) + CINT2(I) + CINT3(I) - RADIAL/WAKE   )*  YV320190
   1SINF(THETAB(I))/2.0                                                 YV320200
    DO 49 I=2,N1                                                        YV320210
 49 THETAB(I-1) = THETAB(I)                                             YV320220
    N2 = N-2                                                            YV320230
    CALL DISCOT (0.0,0.0,THETAB,CPRIME,CPRIME,-020,N2,0,FIRST)          YV320240
    DO 51 I=1,N2                                                        YV320250
    NMINUS = N-I                                                        YV320260
    NLESS = N1-I                                                        YV320270
    THETAB(NMINUS) = THETAB(NLESS)                                      YV320280
 51 CPRIME(NMINUS) = CPRIME(NLESS)                                      YV320290
    THETAB(1) = 0.0                                                     YV320300
    CPRIME(1) = FIRST                                                   YV320310
    CALL DISCOT (PI,PI,THETAB,CPRIME,CPRIME,-020,N1,0,CPRIME(N))        YV320320
    TANA = CPRIME(1) + 4.0*CPRIME(N1) + CPRIME(N)                       YV320330
    DO 52 I=2,NJN,2                                                     YV320340
 52 TANA = TANA + 4.0*CPRIME(I) + 2.0*CPRIME(I+1)                       YV320350
    TANA = DELTA*TANA/3.0
    ATTACK = 57.295780*ATANF(TANA)                                      YV320370
    DO 53 I=1,N                                                         YV320380
 53 CPRIME(I) =-CPRIME(I) + SINF(THETAB(I))*TANA/2.0                    YV320390
    RETURN                                                              YV320400
    END                                                                 YV320410
     FOR                                                                YV33
    SUBROUTINE INTRL2(N1,I,THETAB,H,Z,S,DELTA,THICK,NJN,N,SUMI2,PI)
    DIMENSION THETAB(101),F2(101),THICK(101),STHETA(101),S(21),Z(21)    YV33
    IF(I-2)290,290,291                                                  YV33
290 DO 292 J=2,N1                                                       YV33
    ZTHETA=.5*(1.0+COSF(THETAB(J)))                                     YV33
```

```
292 CALL DISCOT(ZTHETA,ZTHETA,Z,S,S,-130,21,0,STHETA(J))                YV33
291 DO 200 J=2,N1
    IF(I-J)210,211,210
211 F2(J)=0.0                                                            YV33
    GO TO 200                                                            YV33
210 PART=COSF(THETAB(I))-COSF(THETAB(J))                                 YV33
    PARTH=.5*H*PART                                                      YV33
    CONK2=SQRTF(1.0/(PARTH**2+1.0))                                      YV33
    CALL CWORK(CONK2,PARTH,EK,EE,DIF)                                    YV33
    F2(J)=STHETA(J)*CONK2**3*PART*DIF*SINF(THETAB(J))                    YV33
200 CONTINUE                                                             YV33
    SUMI2=4.0*F2(N-1)                                                    YV33
    DO 201 J=2,NJN,2                                                     YV33
201 SUMI2=SUMI2+4.0*F2(J)+2.0*F2(J+1)
    SUMI2=.25*H**2*DELTA*SUMI2/3.0                                       YV33
    DO 202 J=1,N
    IF(J-1)250,250,251                                                   YV33
250 F2(J) = -STHETA(I)*SINF(THETAB(I))/(COSF(THETAB(I)) - COSF(THETAB(
   1J)))                                                                 YV33
    GO TO 202                                                            YV33
251 IF(N-J)250,250,252                                                   YV33
252 IF(I-J)253,254,253                                                   YV33
254 F2(J) = THICK(I) + STHETA(I)*COSF(THETAB(I))/SINF(THETAB(I))
    GO TO 202                                                            YV33
253 PART=COSF(THETAB(I))-COSF(THETAB(J))                                 YV33
    PARTH=.5*H*PART
    CONK2=SQRTF(1.0/(PARTH**2+1.0))                                      YV33
    CALL EELLIP(CONK2,EE)                                                YV33
    F2(J)=(STHETA(J)*SINF(THETAB(J))*CONK2**3*EE
   1  - STHETA(I)*SINF(THETAB(I)))/PART
202 CONTINUE                                                             YV33
    STORE=F2(1)+4.0*F2(N-1)+F2(N)                                        YV33
    DO 203 J=2,NJN,2                                                     YV33
203 STORE=STORE+4.0*F2(J)+2.0*F2(J+1)                                    YV33
    STORE= DELTA*STORE/3.0                                               YV33
    SUMI2=-H*(SUMI2+STORE)/PI                                            YV33
    RETURN
    END                                                                  YV33
     FOR                                                                 YV30
    SUBROUTINE INTRL1 (CINT1,DELTA,H,           NJN,NZ,PI,WAKE,WDIFFRYV30
   1,THETA,      N,THETAB,        VDIFR,I)                               YV30
    DIMENSION WDIFFR(37),THETA(37),THETAB(101),F1(101),VDIFR(101)        YV30
    IF (I-2) 202,202,203                                                 YV30
202 DO 212 J=1,N                                                         YV30
212 CALL DISCOT (THETAB(J),THETAB(J),THETA,WDIFFR,WDIFFR,-020,NZ,0       YV30
   1,VDIFR(J))                                                           YV30
203 DO 200 J=1,N                                                         YV30
    IF (I-J) 232,231,232
231 F1(J) = 0.0                                                          YV30
    GO TO 200                                                            YV30
232 PART = COSF(THETAB(I)) - COSF(THETAB(J))
    PARTH = .5*PART*H
    CONK1 = SQRTF(1.0/(PARTH**2 + 1.0))                                  YV30
    CALL CWORK (CONK1,PARTH,EK,EE,DIF)                                   YV30
    F1(J) = VDIFR(J)*PART*CONK1*DIF                                      YV30
200 CONTINUE                                                             YV30
    CINT1 = F1(1) + 4.0*F1(N-1) + F1(N)                                  YV30
    DO 250 I=2,NJN,2                                                     YV30
250 CINT1 = CINT1 + 4.0*F1(I) + 2.0*F1(I+1)                              YV30
    CINT1 =-H**2*DELTA*CINT1/(12.0*PI*WAKE)                              YV30
```

```
      RETURN
      END                                                               YV30 320
       FOR                                                              YV150010
      SUBROUTINE INTGRL (ANGLE ,CONSK,COS1,EE,FB,FIRST,I,II,L,      NN, YV150020
     1NNN,THETA1,THETA5,JJJ,M,H)
      DIMENSION CONSK(101),THETA5(101),EE(101),FB(101)                  YV150040
C LOOP FOR CALCULATION OF INTEGRAND VALUES FOR INTEGRATION WITH         YV150050
C                    RESPECT TO THETA 5                                 YV150060
      DO 101 J=JJJ,NN,JJJ                                               YV150070
      IF (J-JJJ) 800,800,810                                            YV150080
  800 THETA5(J) = FIRST                                                 YV150090
C THETA5 VARIES FROM 0.0 TO PI                                          YV150100
      GO TO 811                                                         YV150110
  810 THETA5(J) = THETA5(J-1) + ANGLE                                   YV150120
  811 DEN = COSF(THETA5(J)) - COS1                                      YV150130
      IF (ABSF(DEN) - 0.000001) 850,850,856                             YV150140
  850 FB(J) = 0.0                                                       YV150170
      GO TO 101                                                         YV150190
  856 CONSK(J) = SQRTF(1.0/(0.25*(H*DEN)**2 + 1.0))                     YV150200
C CALCULATION OF ELLIPTIC CONSTANT K.                                   YV150210
      CALL EELLIP (CONSK(J),EE(J))                                      YV150220
      FB(J) = (1.0 - 1.C/CONSK(J) * EE(J))*(SINF(THETA5(J)))**2/DEN     YV150230
C PARTIAL INTEGRAND VALUE FOR INTEGRATION WITH RESPECT TO THETA5.       YV150240
  101 CONTINUE                                                          YV150250
      RETURN                                                            YV07 850
      END                                                               YV150310
       FOR                                                              YV31  10
      SUBROUTINE MUSK (DELTA,       THETA,WDIFFR,NZ,N,H,NJN,CINT3,THETABYV31  20
     1              ,I,WAKE,PI,VDIFR)
      DIMENSION THETA(37),WDIFFR(37),F3(101),VDIFR(101),THETAB(101)     YV31  40
      DO 10 J=1,N                                                       YV31  50
      IF (I-J) 11,12,11
   12 ABOVE = THETAB(I) + .01
      CALL DISCOT (ABOVE,ABOVE,THETA,WDIFFR,WDIFFR,-020,NZ,0,FAB)       YV31  90
      BELOW = THETAB(I) - .01
      CALL DISCOT (BELOW,BELOW,THETA,WDIFFR,WDIFFR,-020,NZ,0,FBEL)      YV31 110
      F3(J) = (FAB - FBEL)/(.02*SINF(THETAB(I)))
      GO TO 10                                                          YV31 170
   11 DENOM = COSF(THETAB(I))- COSF(THETAB(J))
      CCONK = SQRTF(1.0/(0.25*(H*DENOM)**2 + 1.0))                      YV31 180
      CALL EELLIP (CCONK,EE)                                            YV31 190
      F3(J) = (VDIFR(J)*CCONK*EE - VDIFR(I))/DENOM                      YV31 210
   10 CONTINUE                                                          YV31 220
      CINT3 = F3(1) + 4.0*F3(N-1) + F3(N)                               YV31 230
      DO 40 J= 2,NJN,2                                                  YV31 240
   40 CINT3 = CINT3 + 4.0*F3(J) + 2.0*F3(J+1)                           YV31 250
      CINT3 = DELTA*CINT3/(6.0*PI*WAKE)                                 YV31 260
      RETURN
      END                                                               YV31 320
```

## REFERENCES


1. Kort, L., "Der nine Düsenschraubenantrieg," Werft Reed. Hafen, Vol. 15, pp. 41-43 (1934).

2. Burnell, J.A. and Sacks, A.H., "Ducted Propellers - A Critical Review of the State of the Art," Progress in Aeronautical Sciences, Vol. 3, Pergemon Press, pp. 87-135 (1962).

3. Dickmann, H.E., "Grundlagen zur Theorie ringförmigen Tragflügel (frei umströmte Düsen)," Ingenieur-Archiv, Vol. II (1940), pp. 36-52. (Translation, Polytechnic Institute of Brooklyn, Pibal Report 353).

4. Weissinger, J., "Zur Aerodynamik des Ringflügels, I. Die Druckuerteilung dünner, fast drehsymmetrischer Flügel in Unterschallströmung," Deutsche Versuchsanstalt für Luftfahrt, E.V. Bericht Nr. 2, Mülheim (Sep 1955). (Translation, David Taylor Model Basin, DTMB Aero Memo 899).

5. Weissinger, J., "Einige Ergebnisse aus der Theorie des Ring Flügels in Inkompressibler Stromung," Advances in Aeronautical Sciences, Vol. 2, Pergamon Press, pp. 798-831 (1959).

6. Hough, G.R., "The Aerodynamic Loading on Streamlined Ducted Bodies," THERM, Inc., TAR-TR 625 (Dec 1962).

7. Morgan, W.B. and Caster, E.B., "Prediction of the Aerodynamic Characteristics of Annular Airfoils," David Taylor Model Basin Report 1830 (Jan 1965).

8. Chaplin, H.R., "A Method for Numerical Calculation of Slipstrear Contraction of a Shrouded Impulse Disc in the Static Case with Application to Other Axisymmetric Potential Flow Problems," David Taylor Model Basin Report 1857 (Jan 1964).

9. Morgan, W.B., "Theory of the Annular Airfoil and Ducted Propeller," Fourth Symposium on Naval Hydrodynamics, Office of Naval Research, ACR-93, (1962).

10. Dickmann, H.E. and Weissinger, J., "Beitrag zur Theorie optimaler Düsenschrauben (Kortdüsen)," Jahrbuch Schiffbau Technicken Gesellschaft, Bd. 49, pp. 253-304 (1955).

11. Ryall, D.L. and Collins, I.F., "Design and Test of a Series of Annular Airfoils," Admiralty Research Laboratory Report ARL/R3/G/AE/2/5, ARL/G/R6 (Mar 1965).

12. Oosterveld, M.W.C., "Series of Model Tests of Ducted Propellers," Nederlandsch Scheepsbouwkundig Proefstation Report on Contract No. N62558-3960 (May 1965).

13. Dyne, G., "Dyspropellrar," The Swedish State Shipbuilding Experimental Tank Report No. 16 (1966).

14. Morgan, W.B., "A Theory of the Ducted Propeller with a Finite Number of Blades," University of California, Institute of Engineering Research, Berkeley (May 1961).

15. Muskhelishvili, N.I., "Singular Integral Equations," P. Noordhoff, N.V. Groningen, Holland (1953).

16. Voigt, R.G., "On a Numerical Solution of an Integral Equation with Singularities," Mathematics of Computation, Vol. 20, pp. 163-166 (Jan 1966).

17. Mikhlin, S.G., "Integral Equations," Pergamon Press, New York (1957).

18. Gradshteyn, I.S. and Ryzhik, I.M., "Tables of Series, Products, and Integrals," Bev Deutscher Verlag Der Wissenschaften, Berlin (1963). Also available from Academic Press, 1966.

19. Hough, G.R. and Ordway, D.E., "The Generalized Actuator Disk," Developments in Theoretical and Applied Mechanics, Vol. II, Pergamon Press (1965), pp. 317-336.

20. Abbott, I.H. and von Doenhoff, A.E., "Theory of Wing Sections," Dover Publications, Inc., New York (1958).

BLANK PAGE

UNCLASSIFIED
Security Classification

| DOCUMENT CONTROL DATA - R&D | | |
|---|---|---|
| *(Security classification of title, body of abstract and indexing annotation must be entered when the overall report is classified)* | | |
| 1 ORIGINATING ACTIVITY *(Corporate author)*<br>David Taylor Model Basin<br>Washington, D.C. 20007 | 2a. REPORT SECURITY CLASSIFICATION<br>Unclassified | |
| | 2b GROUP | |
| 3 REPORT TITLE<br>THE INVERSE PROBLEM OF THE ANNULAR AIRFOIL AND DUCTED PROPELLER | | |
| 4. DESCRIPTIVE NOTES *(Type of report and inclusive dates)*<br>Final | | |
| 5 AUTHOR(S) *(Last name, first name, initial)*<br>Morgan, William B. and Voigt, Robert G. | | |
| 6. REPORT DATE<br>September 1966 | 7a. TOTAL NO. OF PAGES<br>56 | 7b. NO. OF REFS<br>20 |
| 8a. CONTRACT OR GRANT NO.<br>b. PROJECT NO. Subproject S-R011 01 01<br>c. Task 0401<br>d. Problem Number 526-352 | 9a. ORIGINATOR'S REPORT NUMBER(S)<br>2251<br>9b. OTHER REPORT NO(S) *(Any other numbers that may be assigned this report)* | |
| 10. AVAILABILITY/LIMITATION NOTICES<br>Distribution of this document is unlimited. | | |
| 11 SUPPLEMENTARY NOTES | 12. SPONSORING MILITARY ACTIVITY<br>Naval Ship Systems Command<br>Washington, D.C. | |

13. ABSTRACT

A computer program is presented that calculates the annular airfoil shape from a given pressure distribution. A brief review of the theory of the inverse problem of the annular airfoil is also presented. The distortion of the duct shape by the presence of an axisymmetric body or a propeller may be taken into consideration. Calculations show that for a given pressure distribution, the propeller loading and location affect the duct shape.

UNCLASSIFIED

Security Classification

| 14. KEY WORDS | LINK A | | LINK B | | LINK C | |
|---|---|---|---|---|---|---|
| | ROLE | WT | ROLE | WT | ROLE | WT |
| Annular Airfoils | | | | | | |
| Ducted Propellers | | | | | | |
| Shrouded Propellers | | | | | | |
| Pressure Distribution | | | | | | |

INSTRUCTIONS

1. ORIGINATING ACTIVITY: Enter the name and address of the contractor, subcontractor, grantee, Department of Defense activity or other organization *(corporate author)* issuing the report.

2a. REPORT SECURITY CLASSIFICATION: Enter the overall security classification of the report. Indicate whether "Restricted Data" is included. Marking is to be in accordance with appropriate security regulations.

2b. GROUP: Automatic downgrading is specified in DoD Directive 5200.10 and Armed Forces Industrial Manual. Enter the group number. Also, when applicable, show that optional markings have been used for Group 3 and Group 4 as authorized.

3. REPORT TITLE: Enter the complete report title in all capital letters. Titles in all cases should be unclassified. If a meaningful title cannot be selected without classification, show title classification in all capitals in parenthesis immediately following the title.

4. DESCRIPTIVE NOTES: If appropriate, enter the type of report, e.g., interim, progress, summary, annual, or final. Give the inclusive dates when a specific reporting period is covered.

5. AUTHOR(S): Enter the name(s) of author(s) as shown on or in the report. Enter last name, first name, middle initial. If military, show rank and branch of service. The name of the principal author is an absolute minimum requirement.

6. REPORT DATE: Enter the date of the report as day, month, year; or month, year. If more than one date appears on the report, use date of publication.

7a. TOTAL NUMBER OF PAGES: The total page count should follow normal pagination procedures, i.e., enter the number of pages containing information.

7b. NUMBER OF REFERENCES: Enter the total number of references cited in the report.

8a. CONTRACT OR GRANT NUMBER: If appropriate, enter the applicable number of the contract or grant under which the report was written.

8b, 8c, & 8d. PROJECT NUMBER: Enter the appropriate military department identification, such as project number, subproject number, system numbers, task number, etc.

9a. ORIGINATOR'S REPORT NUMBER(S): Enter the official report number by which the document will be identified and controlled by the originating activity. This number must be unique to this report.

9b. OTHER REPORT NUMBER(S): If the report has been assigned any other report numbers *(either by the originator or by the sponsor)*, also enter this number(s).

10. AVAILABILITY/LIMITATION NOTICES: Enter any limitations on further dissemination of the report, other than those imposed by security classification, using standard statements such as:

(1) "Qualified requesters may obtain copies of this report from DDC."

(2) "Foreign announcement and dissemination of this report by DDC is not authorized."

(3) "U. S. Government agencies may obtain copies of this report directly from DDC. Other qualified DDC users shall request through ________________."

(4) "U. S. military agencies may obtain copies of this report directly from DDC. Other qualified users shall request through ________________."

(5) "All distribution of this report is controlled. Qualified DDC users shall request through ________________."

If the report has been furnished to the Office of Technical Services, Department of Commerce, for sale to the public, indicate this fact and enter the price, if known.

11. SUPPLEMENTARY NOTES: Use for additional explanatory notes.

12. SPONSORING MILITARY ACTIVITY: Enter the name of the departmental project office or laboratory sponsoring *(paying for)* the research and development. Include address.

13. ABSTRACT: Enter an abstract giving a brief and factual summary of the document indicative of the report, even though it may also appear elsewhere in the body of the technical report. If additional space is required, a continuation sheet shall be attached.

It is highly desirable that the abstract of classified reports be unclassified. Each paragraph of the abstract shall end with an indication of the military security classification of the information in the paragraph, represented as *(TS), (S), (C), or (U)*.

There is no limitation on the length of the abstract. However, the suggested length is from 150 to 225 words.

14 KEY WORDS: Key words are technically meaningful terms or short phrases that characterize a report and may be used as index entries for cataloging the report. Key words must be selected so that no security classification is required. Identifiers, such as equipment model designation, trade name, military project code name, geographic location, may be used as key words but will be followed by an indication of technical context. The assignment of links, roles, and weights is optional.

UNCLASSIFIED

Security Classification